

Technical Report # KU-EC-13-1: Segregation Indices for Disease Clustering

Elvan Ceyhan*

April 8, 2019

Abstract

Spatial clustering has important implications in various fields. In particular, disease clustering is of major public concern in epidemiology. In this article, we propose the use of two distance-based segregation indices to test the significance of disease clustering among subjects whose locations are from a homogeneous or an inhomogeneous population. We derive their asymptotic distributions and compare them with other distance-based disease clustering tests in terms of empirical size and power by extensive Monte Carlo simulations. The null pattern we consider is the random labeling (RL) of cases and controls to the given locations. Along this line, we investigate the sensitivity of the size of these tests to the underlying background pattern (e.g., clustered or homogenous) on which the RL is applied, the level of clustering and number of clusters, or differences in relative abundances of the classes. We demonstrate that differences in relative abundance has the highest impact on the empirical sizes of the tests. We also propose various non-RL patterns as alternatives to the RL pattern and assess the empirical power performance of the tests under these alternatives. We illustrate the methods on two real-life examples from epidemiology.

Keywords: cell-specific tests, Cuzick-Edwards' tests, empirical power, empirical size, nearest neighbor contingency table, overall test, random labeling, spatial clustering

*corresponding author.

e-mail: elceyhan@ku.edu.tr (E. Ceyhan)

1 Introduction

Recently, spatial clustering has become a topic of extensive study in many fields such as geography, ecology, astronomy, and epidemiology. The relevant methodology is discussed in many books such as Ripley (2004) and Diggle (2003); even special issues of journals are devoted to this topic, see, e.g., Banerjee and Dey (2012) and LeSage et al. (2009). In particular, the significance of disease clustering in human or other populations has received considerable attention (Waller and Gotway (2004), Lawson and Denison (2002) and Rogerson (2006)). Roughly speaking, a *disease cluster* is a region or neighborhood where the number of cases substantially exceeds the expected number of cases at a specific time or for a specific time period (Gómez-Rubio et al. (2003)). There are many tests available for testing the significance of disease clustering. Among them are tests for deviation from homogeneity like the usual Pearson's chi-square statistic for quadrat data or Potthoff-Whittinghill's test (Potthoff and Whittinghill (1966)). Clustering methods for detection of disease clustering can be grouped into four categories: (i) methods based on regional count data, (ii) individual point data (e.g., case-control data in epidemiology), (iii) adjacencies of high count regional data, and (iv) distance-based methods. Cuzick-Edwards' k -nearest neighbor (NN) test (Cuzick and Edwards (1990)) is an example of category (ii) and has been frequently employed in epidemiology so that it is suggested in the appendix of guidelines for disease clustering (Centers for Disease Control and Prevention (1990)).

*Department of Mathematics, Koç University, Sarıyer, 34450, Istanbul, Turkey.

Regional count method is the procedure in which a square grid is overlaid over the region of interest and the number of events in each quadrat is counted. Assuming the points are from a homogeneous Poisson process (HPP), which is the null pattern, the quadrat counts would be distributed as Poisson variates, and their departure from the null case can be tested using an index of dispersion (like ratio of variance to mean), or χ^2 test for heterogeneity of the cell counts. This method has various shortcomings, especially for disease clustering. For example, the quadrats would not be square cells, but administrative units determined by geographical limitations or human intervention. This problem can somewhat easily be overcome by extending the quadrat method to other shapes or administrative units by simply using the chi-square goodness-of-fit test using the observed and expected numbers in each region. Other main problems are the arbitrariness in the choice of grid size and obtaining correct expected quadrat counts on a sufficiently fine grid structure (Cuzick and Edwards (1990)).

Statistical methodology based on NN (or distance-based) methods include at least six different groups (Dixon (2002b)). Each of these methods assumes as a premise that similarity or dissimilarity between a point and its NN provides useful information for statistical inference. The most straightforward dissimilarity measure is the distance between a point and its NN, while other methods could be based on classifying the types of points and their NNs. Spatial clustering of points from one class can also be investigated by distance indices. For example, Perry (1998) introduced SADIE (Spatial Analysis by Distance Indices) to detect deviations from randomness for planar data. These indices were designed to utilize count data and two new indices were proposed and a comparative survey was provided for several other indices in the same reference. The two-class version of the methodology was also developed (Perry (1997)), and with this form of SADIE, it would be possible to detect spatial association or interaction between two species or classes. Cuzick and Edwards (1990) proposed a distance-based method which is applicable in a case-control setting and accounts for geographical inhomogeneity in the population density and also overcomes various confounding factors by appropriately choosing the controls (Tango (2007)). Furthermore, in literature, there are spatial clustering tests based on nearest neighbor contingency tables (NNCTs) due to Pielou (1961) and Dixon (1994) in a two-class setting, and due to Dixon (2002a) in a multi-class setting. Various new segregation tests were also proposed by Ceyhan (2010) based on NNCTs. These tests comprise of an overall test, a compound measure of deviation from the null pattern, and cell-specific tests for pairwise comparisons after a significant overall test. Also a ‘coefficient of segregation’ was introduced by Pielou (1961) in a two-class setting, and ‘segregation indices’ were proposed by Dixon (2002a) in a multi-class setting. However, these indices were merely introduced in passing and not studied in detail (e.g., their asymptotic distributions were not derived) nor they were applied for inferential purposes. In this article, we study their distributional properties and also propose their use for testing spatial clustering (especially of cases compared to controls).

Disease clustering methods can also be classified as *general* or *focused* (Besag and Newell (1991) and Tango (1995)). In the former, presence of any cluster over the entire region is of interest, while in the latter presence of a cluster in the vicinity of a given point is investigated. In this article, we are concerned with the first type of clustering. See Tango (2009) for a review on existing disease clustering methods, their advantages and disadvantages. Several indices measure spatial autocorrelation in a given data which could suggest clustering of a disease, e.g., Moran’s I statistic (Moran (1948)) and Geary’s *c* statistic (Geary (1954)). These indices were employed to assess spatial patterns of disease rates and are compared with another index called rank adjacency statistic, *D*, by Walter (1993). Furthermore, there are methods which provide a general clustering measure for the entire study area, such as Whittemore’s statistic (Whittemore et al. (1987)). However, this statistic was shown to be inadequate by Tango (1999), who also proposed a corrected version of it. As the general clustering methods fail to identify localized clusters, the so called *scan statistics* are developed. In these methods, the region is scanned by a rectangular or circular window to detect any anomaly in disease occurrence or intensity. Examples of scan methods are Openshaw’s GAM (Openshaw et al. (1987)), Besag and Newell’s method to detect clusters of size *k*, which comprise of regions containing exactly *k* observed cases (Besag and Newell (1991)), and Kulldorff & Nagarwalla’s scan statistic (Kulldorff and Nagarwalla (1995)). In literature, despite the lack of a comprehensive comparison of many available geographical disease clustering tests, an empirical comparison was performed by Kulldorff et al. (2003) using spatial scan statistic, the maximized excess events test, and the nonparametric *M* statistic. All tests are shown to have good power for detection of disease clusters and the first having good performance in locating disease hot spots.

In literature, clustering not only in space but also in time is of interest, especially with applications in climatology or ecology (Eshel (2012)). This type of clustering called *spatio-temporal clustering* is also of great merit in disease clustering research. Tango suggested an index for disease clustering in time (Tango

(1984)) and this index is assessed in detail for performance to detect disease clustering in time and space by Kryscio and Lefèvre (1991). Several other indices were also proposed in literature to capture spatial patterns and their evolution in time. See, Woillez et al. (2007) for an example in marine biology which measures spatial patterns of fish populations, and Li and Reynolds (1993) for an example in landscape ecology, where a new contagion index was proposed that also corrects for an existing index. Several other indices such as Camargo’s index of evenness, Simpson’s index of evenness, Lloyd’s index of mean crowding, Smith-Wilson index, and dispersion index, a variant of the Shannon diversity index were employed mainly to quantify biodiversity, but were also possibly usable for measuring spatial patterns from evenness to patchiness (Payne et al. (2005)). Gini-style indices were used in health economics to assess the spatial patterns of health workers (Brown (1994)) and to evaluate residential segregation in a social context (Dawkins (2004)).

In this article, we propose the use of Pielou’s coefficient of segregation and Dixon’s segregation indices in detecting disease clustering against the RL of cases and controls to a set of given spatial locations. Dixon’s segregation indices are not bounded for all possible types of NNCTs, hence we also suggest corrected versions of Dixon’s segregation indices which are bounded for all cell counts (zero or positive) in a NNCT. We derive their asymptotic distributions (more specifically asymptotic normality) and compare these tests with various existing tests, namely, Cuzick-Edwards’ k -NN and combined tests, Dixon’s cell-specific and overall tests, type III cell-specific and overall tests in terms of empirical size and power. For the RL, we investigate the effect of the clustering of the background points (on which RL is performed), including the level of clustering and number of clusters, on the empirical sizes of the tests. We also propose various non-RL patterns as alternatives and investigate the power performance of the tests under these alternatives via extensive Monte Carlo simulations. To the author’s knowledge, these null RL patterns and alternative non-RL patterns are investigated for the first time and in fact the non-RL patterns are newly introduced in this article.

We present the null and alternative patterns and construction of NNCTs in Section 2. The two segregation indices for spatial and disease clustering are provided in Section 3, where the asymptotic normality of Pielou’s coefficient of segregation and Dixon’s segregation indices are derived. Other NN-based spatial clustering tests that are used for comparative purposes are discussed in Section 4. We provide an extensive empirical size comparison of these tests under RL of points from various patterns of complete spatial randomness (CSR) or clustering in Section 5, propose four types of non-RL patterns as alternatives and provide empirical power comparison of the tests under these alternatives in Section 6, illustrate the methodology on two real life data sets from epidemiology in Section 7. Discussion and conclusions are provided in Section 8.

2 Preliminaries

2.1 Null and Alternative Patterns

In a case-control setting, the null pattern we consider is

$$H_o : RL,$$

which is the pattern where the class labels (i.e., case or control labels) are randomly assigned to a given set of locations or points. In the two-class setting, deviations from the null hypothesis are towards two major directions, namely, *segregation* and *association*. *Segregation* is the pattern in which NN of an individual is more likely than expected to be of the same class as the individual than to be from a different class. That is, the probability that this individual having a same-class NN is higher than the relative frequency of this class (see, e.g., Pielou (1961)). On the other hand, *association* is the pattern in which NN of an individual is more likely than expected to be from another class than to be of the same class as the individual. That is, the probability that this individual having a NN from another class is higher than the relative frequency of this other class. See Ceyhan (2010) for a more detailed discussion of the null and alternative patterns.

In a case-control setting, segregation of cases from controls would be equivalent to clustering of cases relative to the controls. In other words, segregation of cases would imply a larger level of clustering compared to the level of clustering of the healthy controls in the society. Furthermore, if for some reason controls are segregated, then this would also mean an (indirect) clustering of cases, but, here the underlying dynamics behind the disease clustering would be different. The association of the cases and controls would mean significant lack of disease clustering; moreover, it would mean clustering of points from both classes (i.e.,

		NN			
		class 1	...	class m	total
base	class 1	N_{11}	...	N_{1m}	n_1
	\vdots	\vdots	\ddots	\vdots	\vdots
	class m	N_{m1}	...	N_{mm}	n_m
total		C_1	...	C_m	n

		NN		
		case	control	total
base	case	N_{11}	N_{12}	n_1
	control	N_{21}	N_{22}	n_2
total		C_1	C_2	n

Table 1: The NNCT for m classes (left) and for two classes in a case-control setting (right).

attraction of controls by cases or vice versa). This may not be practical either, hence is not pursued in detail in the rest of the article. However, association could still be relevant to disease clustering in epidemiology in other settings. For example, one class could be the ‘sources’ of a contaminant or some other pollutant or disease-causing agent, and the other class could be the ‘cases’. The accumulation of cases around the sources more often than expected would mean clustering of a disease around these sources, which is a form of association between the classes. But we will not pursue this type of association in this article either.

2.2 Construction of NNCTs

The segregation indices and most of the tests we consider for comparative purposes in this article are in some way related to NNCTs. We provide a brief description of NNCTs below, for a more detailed description see, e.g., Ceyhan (2010). In a sample of size n , there are n NN pairs, and each NN pair consists of the point labeled as “base” point and its “NN” point. According to the labels of the base and NN points, NN pairs can be classified into various categories and NNCTs are constructed using these categories. For m classes, we will have a $m \times m$ NNCT whose rows represent class labels of base points and columns represent class labels of the corresponding NN points. In the NNCT, the count in cell (or entry) (i, j) is N_{ij} , which is the number of times the NN of a (base) class i point is from class j . See also Table 1 (left) where C_j is the sum of column j ; i.e., number of times class j points serve as NNs for $j \in \{1, 2, \dots, m\}$ and n_i is the sum of row i ; i.e., number of times class i points serve as base class or size of class i for $i = 1, 2, \dots, m$. In what follows, we adopt the convention that lower case letters represent fixed quantities while upper case letters represent random variables. Notice that in a NNCT-analysis, row sums are assumed to be fixed (i.e., class sizes are given), while column sums are random variables depending on the NN relationship between the classes.

In a case-control setting, we have two classes (i.e., $m = 2$) and we reserve class label 1 for cases, and class label 2 for controls. Hence the case-control setting yields a 2×2 NNCT (see Table 1 (right)).

3 Segregation Indices for Spatial and Disease Clustering

3.1 Pielou’s Coefficient of Segregation

In a two-class setting (i.e., for $k = 2$), Pielou’s coefficient of segregation is defined as

$$S_P = 1 - \frac{N_{12} + N_{21}}{\mathbf{E}[N_{12}] + \mathbf{E}[N_{21}]} \quad (1)$$

where $\mathbf{E}[N_{ij}]$ is the expected value of N_{ij} (Pielou (1961)). Notice that the numerator in the second part of S_P is

$$N_{12} + N_{21} = \sum_{i=1}^n \mathbf{I}(\text{point } i \text{ is from class 1 with a NN from class 2}$$

or point i is from class 2 with a NN from class 1)

where $\mathbf{I}()$ stands for the indicator function. In general a $k \times k$ contingency table may result from two multinomial frameworks: row-wise and overall multinomial frameworks. However for spatial data, we have

a special type of contingency table, namely, NNCT, which requires different dependency structure compared to these frameworks for completely mapped data, which include the locations of all points in the region of interest. Below, we discuss these frameworks for completeness, and when each one would be appropriate for a NNCT-analysis.

3.1.1 The Row-wise Multinomial Framework

In this framework, the rows of a contingency table result from independent multinomial distributions. In particular, in the two-class case, each row has a binomial distribution independent of the other rows (so this framework is also referred to as the *binomial framework*).

Let π_{ij} be the probability of a point from class j serving as NN to a point from class i for $i, j \in \{1, 2\}$. In this framework, we assume that $N_i = n_i$ are given and $N_{ij} \sim \text{BIN}(n_i, \pi_{ij})$, the binomial distribution with n_i independent trials and probability of success being π_{ij} . Hence, in the two-class case, (N_{11}, N_{12}) and (N_{21}, N_{22}) are assumed to be independent and so are the individual trials (which are base—NN pairs). Hence this framework would be appropriate for a NNCT-analysis, provided that we have an independent set of (base-NN) pairs, that is, each (base-NN) pair is independent of other pairs. However, for completely mapped data, this assumption does not hold, due to the inherent spatial dependence (for example, a base point would be more likely to be a NN of its own NN compared to being a NN of an arbitrarily selected point). However, if we have data obtained by sparse sampling, this dependence would be nonexistent or negligible, then this framework would be appropriate for the corresponding NNCT. In what follows, when we say data is from sparse sampling, we also assume that (base-NN) pairs constitute an (almost) independent sample. Thus, under sparse sampling with the binomial framework, we would have (N_{11}, N_{12}) is independent of (N_{21}, N_{22}) , and $N_{ij} \sim \text{BIN}(n_i, \pi_{ij})$. Under the null hypothesis of random assignment of case and control labels to any given point proportional to the class sizes, we would have $N_{11} \sim \text{BIN}(n_1, \nu_1)$, $N_{12} \sim \text{BIN}(n_1, \nu_2)$, $N_{21} \sim \text{BIN}(n_2, \nu_1)$, and $N_{22} \sim \text{BIN}(n_2, \nu_2)$, where ν_i is the population proportion of class i points for $i = 1, 2$. Also under H_o , we have $\mathbf{E}[N_{12}] = n_1\nu_2$ and $\mathbf{E}[N_{21}] = n_2\nu_1$ and so

$$S_P = 1 - \frac{N_{12} + N_{21}}{\mathbf{E}[N_{12}] + \mathbf{E}[N_{21}]} = 1 - \frac{N_{12} + N_{21}}{n_1\nu_2 + n_2\nu_1}.$$

We also have $\mathbf{E}[S_P] = 0$, since $\mathbf{E}[N_{12} + N_{21}] = \mathbf{E}[N_{12}] + \mathbf{E}[N_{21}]$ by linearity of expectation. Furthermore, $\mathbf{Var}[N_{ij}] = n_i\pi_{ij}(1 - \pi_{ij})$, so under H_o , $\mathbf{Var}[N_{12}] = n_1\nu_1\nu_2$ and $\mathbf{Var}[N_{21}] = n_2\nu_1\nu_2$, and N_{12} and N_{21} are independent. Hence $\mathbf{Var}[S_P] = \frac{n\nu_1\nu_2}{(n_1\nu_2 + n_2\nu_1)^2}$. However, in practice ν_i would be unknown, and hence need to be estimated. Given sample of size n_i from class i , we estimate ν_i as $\hat{\nu}_i = n_i/n$ for $i = 1, 2$. Then for large n_i , $\mathbf{E}[N_{12}] \approx n_1n_2/n$ and $\mathbf{E}[N_{21}] \approx n_2n_1/n$, so $S_P \approx 1 - \frac{N_{12} + N_{21}}{(2n_1n_2/n)}$. Furthermore, we have $\mathbf{Var}[S_P] \approx \frac{n}{4n_1n_2}$. Then for large n_i , $i = 1, 2$, under sparse sampling, $S_P/\sqrt{\mathbf{Var}[S_P]}$ approximately has $N(0, 1)$ distribution where $N(\mu, \sigma)$ stands for normal distribution with mean μ and standard deviation σ .

3.1.2 The Overall Multinomial Framework

An alternative modeling of a contingency table in general is that cell counts (or the entries) are assumed to arise from multinomial trials. That is, in the two-class case,

$$\mathbf{N} = (N_{11}, N_{12}, N_{21}, N_{22}) \sim \mathcal{M}(n, \nu_1\kappa_1, \nu_1\kappa_2, \nu_2\kappa_1, \nu_2\kappa_2)$$

where $\nu_1 + \nu_2 = 1$ and $\kappa_1 + \kappa_2 = 1$; hence the name *overall multinomial framework*. As in the row-wise multinomial framework, this framework would be appropriate for a NNCT-analysis, provided we have sparsely sampled data. In this framework, $N_{12} \sim \text{BIN}(n, \nu_1\kappa_2)$ and $N_{21} \sim \text{BIN}(n, \nu_2\kappa_1)$. Using $\kappa_2 = 1 - \kappa_1$ and $\nu_2 = 1 - \nu_1$, we have $N_{12} \sim \text{BIN}(n, \nu_1(1 - \kappa_1))$ and $N_{21} \sim \text{BIN}(n, (1 - \nu_1)\kappa_1)$. Hence $\mathbf{E}[N_{12}] = n\nu_1(1 - \kappa_1)$ and $\mathbf{E}[N_{21}] = n(1 - \nu_1)\kappa_1$, which yields $\mathbf{E}[N_{12}] + \mathbf{E}[N_{21}] = n(\nu_1 + \kappa_1) - 2n\nu_1\kappa_1$. Thus it follows that

$$S_P = 1 - \frac{N_{12} + N_{21}}{n(\nu_1 + \kappa_1) - 2n\nu_1\kappa_1}.$$

Furthermore,

$$\mathbf{Var}[N_{12}] = n\nu_1(1 - \kappa_1)(1 - \nu_1 + \nu_1\kappa_1), \quad \mathbf{Var}[N_{21}] = n(1 - \nu_1)\kappa_1(1 - \kappa_1 + \nu_1\kappa_1),$$

and

$$\mathbf{Cov}[N_{12}, N_{21}] = -n\nu_1\kappa_2\nu_2\kappa_1 = -n\nu_1(1 - \kappa_1)(1 - \nu_1)\kappa_1.$$

So $\mathbf{Var}[N_{12} + N_{21}] = n(1 - \nu_1 - \kappa_1 + 2\nu_1\kappa_1)(\nu_1 + \kappa_1 - 2\nu_1\kappa_1)$, which implies $\mathbf{Var}[S_P] = \frac{1 - \nu_1 - \kappa_1 + 2\nu_1\kappa_1}{n(\nu_1 + \kappa_1 - 2\nu_1\kappa_1)}$. Under H_o , we have $\nu_1 = \kappa_1$, and so

$$\mathbf{Var}[S_P] = \frac{1}{2n} \left(\frac{\nu_2}{\nu_1} + \frac{\nu_1}{\nu_2} \right).$$

Hence for large n_i , $i = 1, 2$, $\mathbf{Var}[S_P] \approx \frac{1}{2n} \left(\frac{n_2}{n_1} + \frac{n_1}{n_2} \right)$ and under sparse sampling $S_P / \sqrt{\mathbf{Var}[S_P]}$ approximately has $N(0, 1)$ distribution.

Remark 3.1. Both of the above multinomial frameworks require that we have an independent sample of n (base,NN) pairs, which is approximately valid when we have sparse sampling. However, in a case-control setting, sparse sampling may not be a feasible procedure, especially when the disease in question is rare. Hence, sparse sampling in general is not advisable for detection of disease clustering. However, these frameworks would work when there is a substantial amount of data from both classes in the region of interest, and sparse sampling is a feasible practice to capture the actual interaction between the classes. \square

3.1.3 Pielou's Coefficient of Segregation under RL

Under RL of n_1 cases and n_2 controls to $n = n_1 + n_2$ given locations, we have $\mathbf{E}[N_{12}] = \mathbf{E}[N_{21}] = \frac{n_1 n_2}{n-1}$. So under H_o ,

$$S_P = 1 - \frac{N_{12} + N_{21}}{n_1 n_2 / (n-1)}$$

and $\mathbf{E}[S_P] = 0$. Furthermore,

$$\mathbf{Var}[N_{ij}] = n p_{ij} + Q p_{iij} + (n^2 - 3n - Q + R) p_{iijj} - (n p_{ij})^2,$$

and

$$\mathbf{Cov}[N_{ij}, N_{ji}] = R p_{ij} + (n - R)(p_{iij} + p_{ijj}) + (n^2 - 3n - Q + R) p_{iijj} - n^2 p_{ij} p_{ji},$$

where $p_{ij} = \frac{n_i n_j}{n(n-1)}$, $p_{iij} = \frac{n_i(n_i-1)n_j}{n(n-1)(n-2)}$, $p_{ijj} = \frac{n_i n_j(n_j-1)}{n(n-1)(n-2)}$, and $p_{iijj} = \frac{n_i(n_i-1)n_j(n_j-1)}{n(n-1)(n-2)}$, for $(i, j) = (1, 2)$ and $(i, j) = (2, 1)$, R is twice the number of reflexive pairs and Q is the number of points with shared NNs, which occurs when two or more points share a NN. Then $Q = 2(Q_2 + 3Q_3 + 6Q_4 + 10Q_5 + 15Q_6)$ where Q_k is the number of points that serve as a NN to other points k times. Then $\mathbf{Var}[N_{12} + N_{21}] = \mathbf{Var}[N_{12}] + \mathbf{Var}[N_{21}] + 2\mathbf{Cov}[N_{12}, N_{21}]$, and for large n_i , $S_P / \sqrt{\mathbf{Var}[S_P]}$ has approximately $N(0, 1)$ distribution.

If we have the population proportion, ν_i , for class i , $i = 1, 2$, then we would have, for large n_i , $\mathbf{E}[N_{12}] = \mathbf{E}[N_{21}] \approx n\nu_1\nu_2$ and $S_P \approx 1 - \frac{N_{12} + N_{21}}{n\nu_1\nu_2}$. Furthermore, $p_{ij} = \nu_i\nu_j$, $p_{iij} = \nu_i^2\nu_j$, $p_{ijj} = \nu_i\nu_j^2$, and $p_{iijj} = \nu_i^2\nu_j^2$; hence

$$\mathbf{Var}[N_{ij}] \approx n\nu_i\nu_j + Q\nu_i^2\nu_j + (-3n - Q + R)\nu_i^2\nu_j^2, \quad (2)$$

and

$$\mathbf{Cov}[N_{ij}, N_{ji}] \approx R\nu_i\nu_j + (n - R)(\nu_i^2\nu_j + \nu_i\nu_j^2) + (-3n - Q + R)\nu_i^2\nu_j^2,$$

for $(i, j) = (1, 2)$ and $(i, j) = (2, 1)$.

3.2 Dixon's Segregation Indices

In a multi-class setting, Dixon (2002a) proposed the following indices which are similar to the log odds-ratios in a NNCT:

$$S_{ij}^D = \begin{cases} \log \left(\frac{N_{ii}/(n_i - N_{ii})}{(n_i - 1)/(n - n_i)} \right) & \text{if } i = j, \\ \log \left(\frac{N_{ij}/(n_i - N_{ij})}{n_j/(n - n_j - 1)} \right) & \text{if } i \neq j. \end{cases} \quad (3)$$

For Dixon's segregation index, we will only consider the RL as the underlying framework for the null model. Under RL of n_1 cases and n_2 controls to n given locations, as n_1 and n_2 go to infinity, $(N_{ii} - \mathbf{E}[N_{ii}]) / \sqrt{\mathbf{Var}[N_{ii}]}$ converges in law to $N(0, 1)$ distribution and $(N_{ij} - \mathbf{E}[N_{ij}]) / \sqrt{\mathbf{Var}[N_{ij}]}$ converges in law to $N(0, 1)$ distribution.

Theorem 7.7.6 in Bain and Engelhardt (1992) states that “If $\frac{\sqrt{n}(Y_n-s)}{c} \xrightarrow{\mathcal{L}} N(0, 1)$ and if $g(y)$ has a nonzero derivative at $y = s$, i.e., $g'(s) \neq 0$, then $\frac{\sqrt{n}(g(Y_n)-g(s))}{|cg'(s)|} \xrightarrow{\mathcal{L}} N(0, 1)$ ” where $\xrightarrow{\mathcal{L}}$ stands for “converges in law”. So for $i = j$, letting $s = \frac{n_i(n_i-1)}{n-1}$ and $g(y) = \log(y/(n_i - y))$ so that $g'(s) = \frac{(n-1)^2}{n_i(n-n_i)(n_i-1)} \neq 0$ provided $n > 1$, by the above theorem, we get

$$\frac{\log\left(\frac{N_{ii}}{n_i - N_{ii}}\right) - \log\left(\frac{n_i-1}{n-n_i}\right)}{\sqrt{\mathbf{Var}[N_{ii}]}\left(\frac{(n-1)^2}{n_i(n-n_i)(n_i-1)}\right)} = \frac{S_{ii}^D}{\sqrt{\mathbf{Var}[N_{ii}]}\left(\frac{(n-1)^2}{n_i(n-n_i)(n_i-1)}\right)}$$

approximately having $N(0, 1)$ distribution for large n_i .

Similarly for $i \neq j$, letting $s = \frac{n_i n_j}{n-1}$ we get $g'(s) = \frac{(n-1)^2}{n_i n_j (n-n_j-1)} \neq 0$ provided $n > 1$. By the above theorem, we get

$$\frac{\log\left(\frac{N_{ij}}{n_i - N_{ij}}\right) - \log\left(\frac{n_j}{n-n_j-1}\right)}{\sqrt{\mathbf{Var}[N_{ij}]}\left(\frac{(n-1)^2}{n_i n_j (n-n_j-1)}\right)} = \frac{S_{ij}^D}{\sqrt{\mathbf{Var}[N_{ij}]}\left(\frac{(n-1)^2}{n_i n_j (n-n_j-1)}\right)}$$

approximately having $N(0, 1)$ distribution for large n_i .

For the asymptotic approximations of Dixon’s segregation indices when the population proportion, ν_i , of class i , $i = 1, 2$, are known, see the Appendix section.

3.3 A Correction for Dixon’s Segregation Index

Dixon’s segregation indices may be unbounded in either direction depending on the cell counts in the NNCT. Let $0 < n_i < n$ for all i . Then if $N_{ii} = 0$, we get $S_{ii}^D = -\infty$ provided $n_i > 1$; and if $N_{ij} = 0$, we get $S_{ij}^D = -\infty$ provided $n_j < n - 1$. Also, if $N_{ii} = n_i$, we get $S_{ii}^D = \infty$; and if $N_{ij} = n_i$, we get $S_{ij}^D = \infty$ provided $n_j < n - 1$. To make the segregation indices bounded for all possible cell counts, we suggest the following corrected versions:

$$S_{ij}^{D,c} = \begin{cases} \log\left(\frac{(N_{ii}+1)/(n_i - N_{ii} + 1)}{(n(n_i-1) + (n-1))/(n_i(n-n_i) + (n-1))}\right) & \text{if } i = j, \\ \log\left(\frac{(N_{ij}+1)/(n_i - N_{ij} + 1)}{(n_i n_j + n - 1)/(n_i(n-n_j-1) + (n-1))}\right) & \text{if } i \neq j, \end{cases} \quad (4)$$

where denominators are chosen in this way to have simpler asymptotic approximations for the corrected versions.

For the derivation of asymptotic distribution of these corrected versions, see the Appendix section.

4 Other NN-Tests for Spatial Clustering

Although there are many tests for spatial clustering of points from one class or multiple classes in the literature (Diggle (2003) and Kulldorff (2006)), one-class tests are not comparable with the segregation indices nor very useful in disease clustering. Some of the tests like Moran’s I and Whittemore’s tests are shown to perform poorly in detection of some kind of clustering (Song and Kulldorff (2003)) and most of the tests require Monte Carlo simulation or randomization methods to attach significance to their results. Hence we only consider cell-specific and overall NNCT-tests due to Dixon (1994) and Ceyhan (2010) and Cuzick-Edward’s k -NN tests and their combined versions (Cuzick and Edwards (1990)), and compare the segregation indices with these tests in an extensive Monte Carlo simulation study in terms of size and power performance.

4.1 Cell-Specific and Overall Segregation Tests based on NNCTs

Dixon’s cell-specific and overall tests (Dixon (1994)) and type III cell-specific and overall tests (Ceyhan (2010)) are based on NNCTs. These tests are discussed in detail in Ceyhan (2012); here we only provide a

brief description for completeness. For cell (i, j) , Dixon (1994) suggests

$$Z_{ij}^D = \frac{N_{ij} - \mathbf{E}[N_{ij}]}{\sqrt{\mathbf{Var}[N_{ij}]}} \quad (5)$$

as the cell-specific tests, where under RL the expected cell counts are $\mathbf{E}[N_{ij}] = n_i(n_i - 1)/(n - 1)\mathbf{I}(i = j) + n_i n_j/(n - 1)\mathbf{I}(i \neq j)$ and the variance $\mathbf{Var}[N_{ij}]$ is given in Ceyhan (2010). In the multi-class case with m classes, combining the m^2 cell-specific tests, Dixon (2002a) suggests the following quadratic form as an overall test:

$$C_D = (\mathbf{N} - \mathbf{E}[\mathbf{N}])' \Sigma_D^{-1} (\mathbf{N} - \mathbf{E}[\mathbf{N}]) \quad (6)$$

where \mathbf{N} is the $m^2 \times 1$ vector of m rows of the NNCT concatenated row-wise, $\mathbf{E}[\mathbf{N}]$ is the vector of $\mathbf{E}[N_{ij}]$, Σ_D is the $m^2 \times m^2$ variance-covariance matrix for the cell count vector \mathbf{N} with diagonal entries being equal to $\mathbf{Var}[N_{ij}]$ and off-diagonal entries being $\mathbf{Cov}[N_{ij}, N_{kl}]$ for $(i, j) \neq (k, l)$. The explicit forms of the variance and covariance terms are provided in Dixon (2002a). Also, Σ_D^{-1} is a generalized inverse of Σ_D (Searle (2006)) and $'$ stands for the transpose of a vector or matrix. Then under RL, C_D approximately has a $\chi_{m(m-1)}^2$ distribution for large n_i .

On the other hand, type III cell-specific test suggested by Ceyhan (2010) for cell (i, j) is

$$Z_{ij}^{III} = \frac{T_{ij}^{III}}{\sqrt{\mathbf{Var}[T_{ij}^{III}]}} \quad (7)$$

where $T_{ij}^{III} = \left(N_{ii} - \frac{(n_i-1)}{(n-1)}C_i\right)\mathbf{I}(i = j) + \left(N_{ij} - \frac{n_i}{(n-1)}C_j\right)\mathbf{I}(i \neq j)$. The explicit forms of expectation and variance of T_{ij}^{III} are presented in Ceyhan (2012). We obtain the type III overall test by combining the type III cell-specific tests. Let \mathbf{T}^{III} be the vector of m^2 T_{ij}^{III} values, i.e.,

$$\mathbf{T}^{III} = (T_{11}^{III}, T_{12}^{III}, \dots, T_{1m}^{III}, T_{21}^{III}, T_{22}^{III}, \dots, T_{2m}^{III}, \dots, T_{mm}^{III})'$$

and let $\mathbf{E}[\mathbf{T}^{III}]$ be the vector of $\mathbf{E}[T_{ij}^{III}]$ values. Note that $\mathbf{E}[\mathbf{T}^{III}] = \mathbf{0}$ where $\mathbf{0}$ is the vector of m^2 zeros. As the type III overall segregation test, we use the following quadratic form:

$$C_{III} = (\mathbf{T}^{III})' \Sigma_{III}^{-1} (\mathbf{T}^{III}) \quad (8)$$

where Σ_{III} is the $m^2 \times m^2$ variance-covariance matrix of \mathbf{T}^{III} . Under RL, the explicit forms of the variance-covariance matrix are provided in Ceyhan (2012). Furthermore, under RL, C_{III} approximately has a $\chi_{(m-1)^2}^2$ distribution for large n_i .

4.2 Cuzick-Edwards' k -NN and Combined Tests

For disease clustering, Cuzick and Edwards (1990) suggested a k -NN test based on number of cases among k NNs of the case points. Let z_i be the i^{th} point and d_i^k be the number cases among k NNs of z_i . Then Cuzick-Edwards' k -NN test is $T_k = \sum_{i=1}^n \delta_i d_i^k$, where

$$\delta_i = \begin{cases} 1 & \text{if } z_i \text{ is a case,} \\ 0 & \text{if } z_i \text{ is a control.} \end{cases} \quad (9)$$

Since in practice, the correct choice of k is not known, Cuzick and Edwards (1990) also suggest combining various T_k tests. Let $S = \{k_1, k_2, \dots, k_m\}$ be a set of indices for k , and assume T_k with $k \in S$ being a mixture of shifts all in the same direction under an alternative. Assuming further that T_k has multivariate normal distribution, the combined test statistic is given by

$$T_S = \mathbf{1}' \Sigma^{-1/2} \mathbf{T} \quad (10)$$

where $\mathbf{T} = (T_{k_1}, T_{k_2}, \dots, T_{k_m})'$ (i.e., T_S is the test obtained by combining T_k tests whose indices are in S), $\mathbf{1}' = (1, 1, \dots, 1)$, $\Sigma = \mathbf{Cov}[\mathbf{T}]$ is the variance-covariance matrix of \mathbf{T} . Under RL of n_1 cases and n_2 controls to the given locations in the study region, T_k approximately has $N(\mathbf{E}[T_k], \mathbf{Var}[T_k]/n_1)$ distribution for large

n_1 ; similarly, T_S approximately has $N(\mathbf{E}[T_S], \mathbf{Var}[T_S])$ distribution for large n_1 . The expected values $\mathbf{E}[T_k]$ and $\mathbf{E}[T_S]$ and variances $\mathbf{Var}[T_k]$ and $\mathbf{Var}[T_S]$ are provided in Cuzick and Edwards (1990).

Notice that T_1 is identical to the count for cell (1,1) in the NNCT of Table 1 (right). Hence the corresponding tests $(T_1 - \mathbf{E}[T_1])/\sqrt{\mathbf{Var}[T_1]}$ and Z_{11}^D are identical. Hence, we only consider T_2 and T_S with $S = \{1, 2\}$ for Cuzick-Edwards' tests in our comparisons.

Remark 4.1. Note that under H_o , expected values of $S_P, S_{ii}^D, Z_{ii}^D, T_k - \mathbf{E}[T_k]$ and $T_S - \mathbf{E}[T_S]$ are all zero. However they tend to be positive under segregation and negative under association. On the other hand, under segregation, the diagonal cell counts, N_{ii} , would be larger, while under association, the off-diagonal cell counts, N_{ij} , with $i \neq j$, would be larger than expected. Hence S_{ij}^D and Z_{ij}^D for $i \neq j$ tend to be negative under segregation and positive under association. Hence all these tests can be employed to test spatial clustering in the two directions against H_o in a two-class setting. In a case-control setting, segregation of cases from the controls would be our primary interest. \square

Remark 4.2. With $m = 2$ classes (or in a case-control setting), $S_P, S_{ii}^D, Z_{ii}^D, C_D, T_1$ and C_{III} can detect the spatial interaction at small scales (at around the average NN distance), while T_k with $k > 1$ can detect at larger scales (at around k -th NN distance), and so can T_S with S having indices other than 1 (at around ℓ -th NN distance with $\ell = \min k_i$ to $\ell = \max k_i$ for $k_i \in S$). Hence, $S_P, S_{ii}^D, Z_{ii}^D, C_D, T_1$ and C_{III} can be used to test the same type of interaction at the same scales, but Cuzick-Edwards' tests can be used to do the same at higher scales. \square

5 Empirical Size Analysis of the Tests

Let $\mathcal{Z}_n = \{Z_1, Z_2, \dots, Z_n\}$ be the given set of locations for n points (called *background pattern*). We consider RL of cases and controls to points, \mathcal{Z}_n , generated from various homogeneous or clustered patterns. To remove the effect of one particular realization of the Z_i points on the tests, we consider 100 different realizations of \mathcal{Z}_n on which RL will be applied. For each background realization, we label n_1 of the points as class X (for cases) and the remaining $n_2 = n - n_1$ points as class Y (for controls).

Types of the Background Patterns:

Case 1: We generate \mathcal{Z}_n points independently uniformly in the unit square $(0, 1) \times (0, 1)$, i.e., $Z_i \stackrel{iid}{\sim} \mathcal{U}((0, 1) \times (0, 1))$ for $i = 1, 2, \dots, n$. We consider (a) $n_1 = n_2 = 10, 20, \dots, 100$ to determine the effect of increasing but equal sample sizes, (b) $n_1 = 30$ and $n_2 = 30, 40, \dots, 120$ to determine the differences in the sample sizes with number of cases fixed and number of controls increasing, and (c) $n_2 = 30$ and $n_1 = 30, 40, \dots, 120$ to determine the differences in the sample sizes with number of controls fixed and number of cases increasing. We perform the above RL 1000 times for each (n_1, n_2) combination at each background realization.

Case 2: We generate $Z_i \stackrel{iid}{\sim} \mathcal{U}(S_\delta^I)$ for $i = 1, 2, \dots, n$ where $S_\delta^I = ((0, 1) \times (0, 1)) \cup ((\delta, 1 + \delta) \times (\delta, 1 + \delta))$. We consider $\delta = 0.2, 0.4, \dots, 2.0$, so that as δ increases, the level of clustering of background points increases. We perform the above RL 1000 times for each δ at each background realization with $n_1 = n_2 = 100$.

Case 3: We generate $Z_i \stackrel{iid}{\sim} \mathcal{U}(S_\delta^{II})$ for $i = 1, 2, \dots, n$ where $S_\delta^{II} = ((0, 1) \times (0, 1)) \cup ((1 + \delta, 2 + \delta) \times (0, 1))$. We consider $\delta = 0.0, 0.2, 0.4, \dots, 1.4$, so that as δ increases, the level of clustering of background patterns increases. We perform the above RL 1000 times for each δ at each background realization with $n_1 = n_2 = 100$.

Case 4: We generate $Z_i \stackrel{iid}{\sim} \mathcal{U}(S_{\delta,k})$ for $i = 1, 2, \dots, n$ where $S_{\delta,k} = ((0, 1) \times (0, 1)) \cup ((1 + \delta, 2 + \delta) \times (0, 1)) \dots \cup ((k - 1)(1 + \delta), k + (k - 1)\delta) \times (0, 1))$ which yields k squares along the x -axis for the support of Z_i , with successive squares being δ units apart. We consider $\delta = 0.5$, so that each square is clearly separated, and $k = 1, 2, \dots, 10$ so that the sensitivity of the empirical sizes of the tests to the number distinct clusters could be assessed. We perform the above RL 1000 times for each k at each background realization with $n_1 = n_2 = 100$.

Case 5: In this case, we generate Z_i points from Matérn's cluster process in the unit square, denoted $\text{MatClust}(\kappa, r, \mu)$ (Baddeley and Turner (2005)). First we generate "parent" points from a Poisson

process with intensity κ and then each parent is replaced by N points independently uniformly generated inside the circle centered at the parent point with radius r , where $N \sim \text{Poisson}(\mu)$. For each background realization, we generate one realization of \mathcal{Z}_n from $\text{MatClust}(\kappa, r, \mu)$, and let n be the number of points in this realization. Then we label $n_1 = \lfloor n/2 \rfloor$ of these points as cases, and $n_2 = n - n_1$ as controls, where $\lfloor x \rfloor$ stands for the floor of x . Here we take $\kappa = 1, 2, \dots, 10$, $\mu = \lfloor 200/\kappa \rfloor$, and $r = 0.1$ in our simulations. That is, we take $(\kappa, \mu) \in \{(1, 200), (2, 100), (3, 66) \dots, (10, 20)\}$, so that on the average we would have about 200 Z points of which 100 are X and 100 are Y points.

At each Monte Carlo replication in each of the above cases, we compute the following test statistics: Pielou's coefficient of segregation, S_P , Dixon's segregation indices, S_{ij}^D , for $i, j = 1, 2$, and the corrected versions, $S_{ij}^{D,c}$, for $i, j = 1, 2$, Dixon's cell-specific tests, Z_{ij}^D , for $i, j = 1, 2$ type III cell-specific tests, Z_{ij}^{III} , for $i, j = 1, 2$, Dixon's overall test, C_D , type III overall test, C_{III} , Cuzick-Edwards' k -NN tests, T_k , for $k = 1, 2$, and combined test, T_S , for $S = \{1, 2\}$ (which is denoted as $T_{1,2}$ in short). However, the case-control setting corresponds to a two-class case. Hence in our further analysis, we only consider and present S_{ii}^D for $i = 1, 2$ among Dixon's segregation indices, since $S_{11}^D = -S_{12}^D$ and $S_{22}^D = -S_{21}^D$; Z_{ii}^D for $i = 1, 2$ among Dixon's cell-specific tests, since $Z_{11}^D = -Z_{12}^D$ and $Z_{22}^D = -Z_{21}^D$; Z_{ii}^{III} for $i = 1, 2$ among type III cell-specific tests, since $Z_{11}^{III} = -Z_{21}^{III}$ and $Z_{22}^{III} = -Z_{12}^{III}$. Furthermore, among Cuzick-Edwards' k -NN tests, we only consider and present T_2 , and combined test for $S = \{1, 2\}$, since $(T_1 - \mathbf{E}[T_1])/\sqrt{\mathbf{Var}[T_1]} = Z_{11}^D$ in the two-class case. Also, S_{ij}^D for $i, j = 1, 2$, and the corrected versions, $S_{ij}^{D,c}$ for $i, j = 1, 2$ provide very similar empirical size estimates, hence only the former are presented. In our empirical size analysis (and also in the power analysis in Section 6), we use standardized forms of Pielou's coefficient of segregation and Cuzick-Edwards' tests. That is, we use $Z_P = S_P/\mathbf{Var}[S_P]$, and $(T_k - \mathbf{E}[T_k])/\sqrt{\mathbf{Var}[T_k]}$ for $k = 1, 2$, and $(T_S - \mathbf{E}[T_S])/\sqrt{\mathbf{Var}[T_S]}$ for $S = \{1, 2\}$.

In case 1, we have the background pattern from a HPP; i.e., each realization of \mathcal{Z}_n is from the CSR pattern. In this case, we investigate the effect of equal but increasing sample sizes, and differences in the relative abundances (in both directions, with fixed number of cases and increasing number of controls and vice versa). In case 2, we consider an increasing level of clustering along the diagonal $y = x$ with increasing δ , and for $\delta > 1$, the two clusters are disjoint. In case 3, we already have two disjoint clusters along the x -axis, and the level of clustering increases with increasing δ . Hence in cases 2 and 3, the effect of clustering level on the empirical sizes are assessed. In case 4, we already have k disjoint clusters with $\delta = 0.5$ and assess the effect of number of clusters on the empirical sizes. In case 5, we have clusters where the size and location of the clusters are random according to a Matérn clustering process. In this case, we assess the effect of such clustering on the empirical sizes.

In Figures 1-5, we present the empirical size estimates for the right-sided alternative (i.e., towards segregation) and for left-sided alternative (i.e., towards association). The empirical size estimates are computed as follows. For each Monte Carlo replication, test statistics are computed and the size is estimated based on the asymptotic critical values. For Pielou's coefficient of segregation, Dixon's segregation indices, Dixon's cell-specific tests, type III cell-specific tests, and Cuzick-Edwards' k -NN and combined tests we use the critical value $z_{.95} = 1.96$ for the right-sided (clustering or segregation) alternative and $z_{.05} = -1.96$ for the left-sided (association) alternative. For example, the empirical size of S_P is calculated for the right-sided alternative as $\sum_{i=1}^{N_{mc}} \mathbf{I}(Z_{P,i} > 1.96)$ where we have 1000 Monte Carlo replications for each of background realizations, and since there are 100 different realizations, we would have $N_{mc} = 100000$ and $Z_{P,i}$ is the standardized version of Pielou's coefficient of segregation. On the other hand, for Dixon's overall test, we use 95th percentile of χ_1^2 distribution, which is $\chi_{1,.95}^2 = 3.84$ and for type III overall test, we use $\chi_{2,.95}^2 = 5.99$.

The empirical significance levels under cases 1(a)-(c) for the right-sided and left-sided alternatives are presented in Figures 1 and 2, respectively. In case 1(a), we have equal but increasing sample sizes (i.e., $n_1 = n_2 = n/2 = 10, 20, \dots, 100$), and as expected the size performance gets better (i.e., empirical size approaches to the nominal size of 0.05) as n increases. Furthermore, all the tests have empirical size estimates around the null region (i.e., between .04887 and .05113). These bounds for the null region are estimated as follows. With $N_{mc} = 100000$, an empirical size estimate larger than .05113 is deemed liberal, while an estimate smaller than .04887 is deemed conservative at .05 level (based on binomial critical values with $n = 100000$ trials and probability of success 0.05). Among the cell-related tests (i.e., cell-specific tests and segregation indices), size estimates of type III test are closer to the nominal level of 0.05, when all the tests considered type III tests, Pielou's test and Cuzick-Edwards' tests have less fluctuation around 0.05, and $T_{1,2}$ is closest to the nominal level and has the least fluctuation. For the left-sided alternative, (i.e., towards association) Dixon's segregation indices are extremely liberal for $n \leq 80$, and Dixon's cell-specific tests and segregation

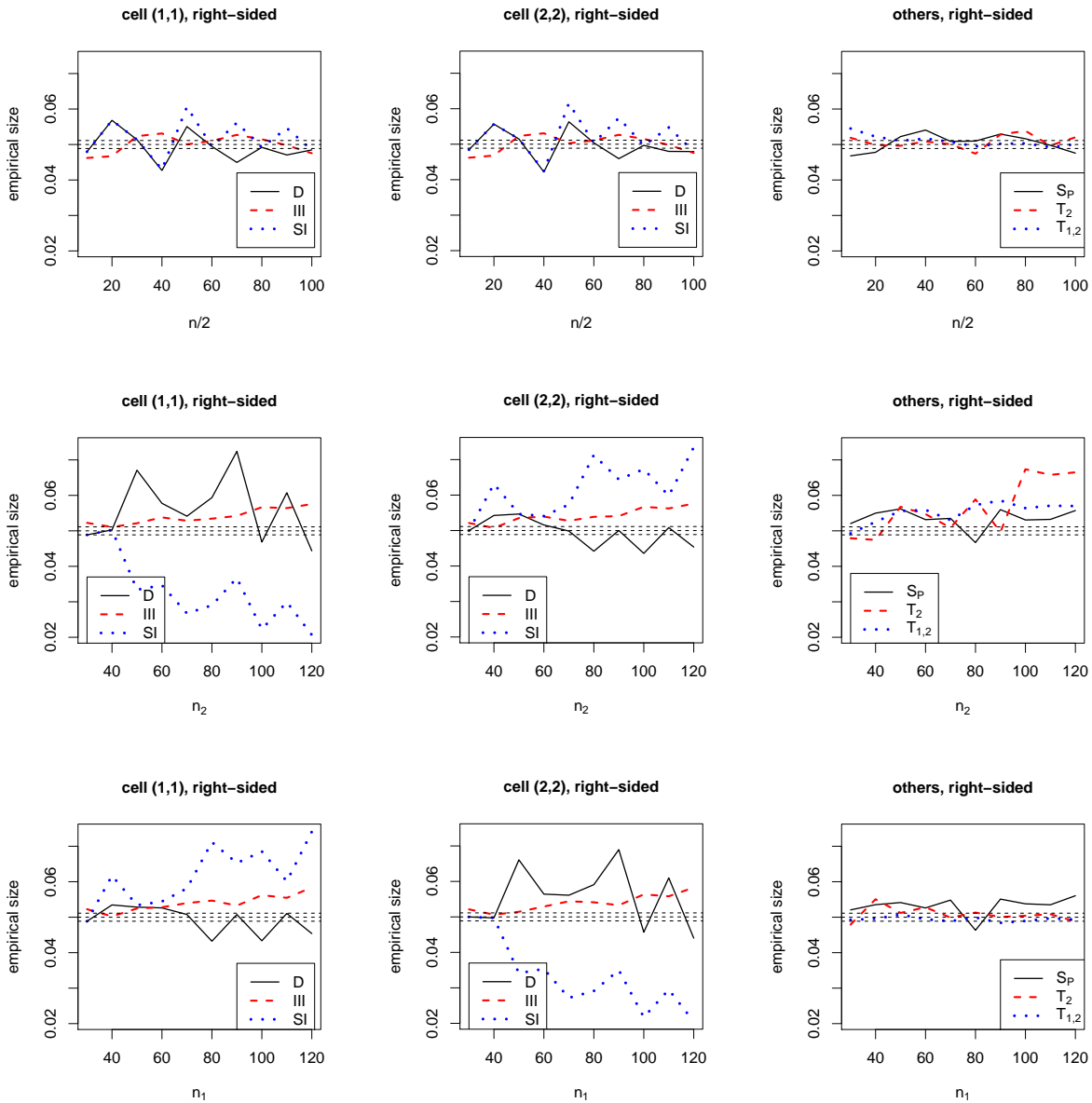


Figure 1: The empirical size estimates for the tests under the RL cases 1(a)-(c) for the right-sided alternative. In case 1(a) (top row), we take $n_1 = n_2 = n/2 = 20, 30, \dots, 100$, in case 1(b) (middle row), we take $n_1 = 30$ and $n_2 = 30, 40, \dots, 100$ and in case 1(c) (bottom row) we take $n_1 = 30, 40, \dots, 100$ and $n_2 = 30$. In the legends, D stands for Dixon's cell-specific tests, III for type III cell-specific tests, SI for Dixon's segregation indices, S_P for Pielou's coefficient of segregation, T_2 for Cuzick-Edwards' 2-NN test, and $T_{1,2}$ for Cuzick-Edwards' combined test, T_S , for $S = \{1, 2\}$. The dashed horizontal lines are at .04887 and .05113, the lower and upper bounds for significant deviation from .05. Also, empirical size estimates for each test are joined by straight lines for better visualization.

indices fluctuate more around 0.05, compared to other tests. Among cell-related tests, type III has the best size performance, but all tests considered, $T_{1,2}$ is closest to the nominal level and has the least fluctuation.

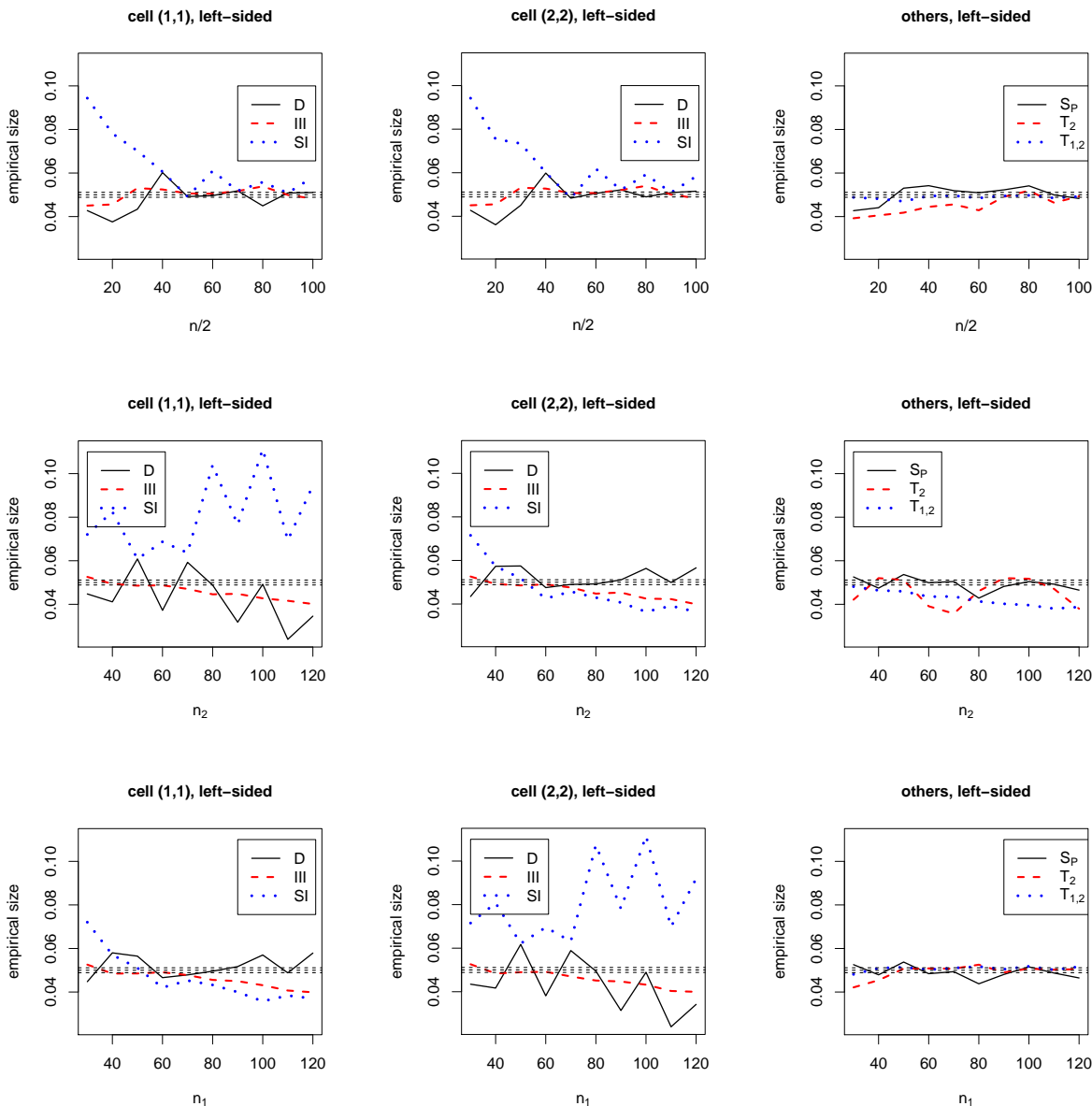


Figure 2: The empirical size estimates for the tests under the RL cases 1(a) (top row), 1(b) (middle row) and 1(c) (bottom row) for the left-sided alternative. The horizontal lines and legend labeling are as in Figure 1.

In case 1(b), we have $n_1 = 30$ and $n_2 = 30, 40, \dots, 120$, i.e., the difference in relative abundance increases as n_2 increases, and in this case, with increasing n_2 the disease incidence rate is decreasing. Hence in this case, we investigate the effect of decreasing incidence rate (starting from 50% and decreasing to 20%) on the empirical sizes. For the right-sided alternatives, among cell (1, 1) statistics, Dixon’s test fluctuates between liberalness and the desired level, Dixon’s segregation index tends to be conservative (with level of conservativeness increasing with n_2), and type III cell-specific statistic is slightly above the null region with its size estimate increasing with n_2 . Among cell (2, 2) statistics, Dixon’s segregation indices tends to be liberal (with level of liberalness increasing with n_2), and type III has the same performance as in cell (1, 1), and Dixon’s cell-specific is closest to the nominal level. S_P , T_1 , and $T_{1,2}$ seem to be generally above the null region, with S_P being closest to .05. All tests considered, Dixon’s cell (2, 2) test and Pielou’s coefficient of segregation have better performance, with S_P having slightly better performance. For the left-sided alternatives, among

cell (1, 1) statistics, Dixon's test fluctuates between conservativeness and the desired level (and tends to get more conservative with increasing n_2), Dixon's segregation index tends to be extremely liberal (although fluctuating, the level of liberalness tends to increase with n_2), and type III statistic is slightly below the null region with its size estimate decreasing with n_2 . Among cell (2, 2) statistics, Dixon's segregation indices have a decreasing trend with increasing n_2 (starting liberal and getting conservative eventually), and type III has the same performance as in cell (1, 1), and Dixon's cell-specific test is closest to the nominal level. T_1 and $T_{1,2}$ are slightly conservative with a clear decreasing trend in size estimate of $T_{1,2}$. On the other hand, S_P is closest the null region. All tests considered, Dixon's cell (2, 2) test and S_P have better performance, with S_P having slightly better performance. Hence, the differences in the relative abundances increasing in favor of controls (i.e., decreasing incidence rate of the disease) confounds most test statistics. Among the tests considered, S_P seems to be the most robust to such differences in sample sizes.

In case 1(c), we have $n_2 = 30$ and $n_1 = 30, 40, \dots, 120$, i.e., the difference in relative abundance increases as n_1 increases, and in this case, with increasing n_1 the disease incidence rate is increasing. Hence in this case, we investigate the effect of increasing incidence rate (starting from 50% and increasing to 80%) on the empirical sizes. The trends in S_P and type III tests are as in case 1(b), with the roles of classes switched, the tests yield the same results for a given data. Furthermore, Dixon's cell (i, i) statistics and segregation indices behave similar to those for cell (j, j) of case 1(b) for $i \neq j$ switching also n_2 with n_1 . For the right-sided and left-sided alternatives, T_2 and $T_{1,2}$ are closest to the null region and have better performance than the other tests (with $T_{1,2}$ having the best performance). Hence, the differences in the relative abundances increasing in favor of cases (i.e., increasing incidence rate of the disease) confounds most test statistics. Among the tests considered, T_2 and $T_{1,2}$ and to a lesser extent S_P seem to be the most robust statistics to such differences in sample sizes and $T_{1,2}$ has the best performance. The better performance of Cuzick-Edwards' tests in this case is no coincidence, since these tests are designed to detect the clustering of cases (i.e., class 1 points), and the number of class 1 points increases in this case.

The empirical size estimates under cases 2-4 for the right-sided and left-sided alternatives are presented in Figures 3 and 4, respectively. In case 2, we have equal sample sizes with $n_1 = n_2 = 100$, but with increasing δ , the level of clustering of the two clusters in the background pattern increases (in fact, with $\delta > 1$, the clusters get separated). For the right-sided alternative, all tests are almost within the null region with Dixon's cell (1, 1) statistics closest to the nominal level. Cell-related tests except Dixon's cell (1, 1) test and S_P tend to be slightly conservative, while Cuzick-Edwards' tests tend to be slightly liberal. For the left-sided alternative, all tests except Dixon's segregation indices are within the null region. Dixon's segregation indices are liberal and has size estimates about 0.06, Dixon's cell-specific tests are slightly liberal, and all other tests are slightly conservative. Hence, with sample sizes are equal and large, most tests are unaffected seriously with increasing level of clustering in the background realizations, and Dixon's segregation indices are most severely confounded with δ . There is no clear (increasing or decreasing) trend in the size estimates of the tests with increasing δ .

In case 3, we have equal sample sizes with $n_1 = n_2 = 100$, but with increasing δ , the level of clustering of the two separated clusters in the background pattern increases. For both alternatives, the empirical size performance of the tests is similar to the performance under case 2. In case 4, we have equal sample sizes with $n_1 = n_2 = 100$, and same separation length $\delta = 0.5$, but the number of clusters in the background pattern increases. For the one-sided alternatives, the empirical size performance of the tests is similar to the performance under case 2. Hence we notice that with sample sizes being equal and large, the sizes of the tests are not affected by the increasing number of clusters in the background realizations.

The empirical size estimates under case 5 for the right-sided and left-sided alternatives are presented in Figure 5. In this case, we have sample sizes $n_1 = n_2 = 100$ on the average, and random number of clusters κ (with increasing κ , the number of clusters tend to increase), and the locations of the clusters are also random. For the right-sided alternative, Dixon's segregation indices, T_2 and $T_{1,2}$ are above 0.05, while other tests are around 0.05. Type III tests, Dixon's cell-specific tests and S_P seem to have the best performance. For the left-sided alternative, Dixon's segregation indices tend to be above 0.05, T_2 and $T_{1,2}$ are below 0.05, while other tests are around 0.05. Type III tests, S_P and $T_{1,2}$ seem to have the best performance. Hence, with randomly occurring and randomly increasing number of clusters, most tests are not affected seriously. Dixon's segregation indices have the worst size performance under RL of this type of background clustering.

The empirical size estimates for overall NNCT-tests under cases 1-5 are presented in Figure 6. In cases 1(a) and 2-5, Dixon's overall test is mostly liberal and around the null region in cases 1(b) and (c). On the other hand, type III overall test is within the null region or slightly conservative, and has better performance

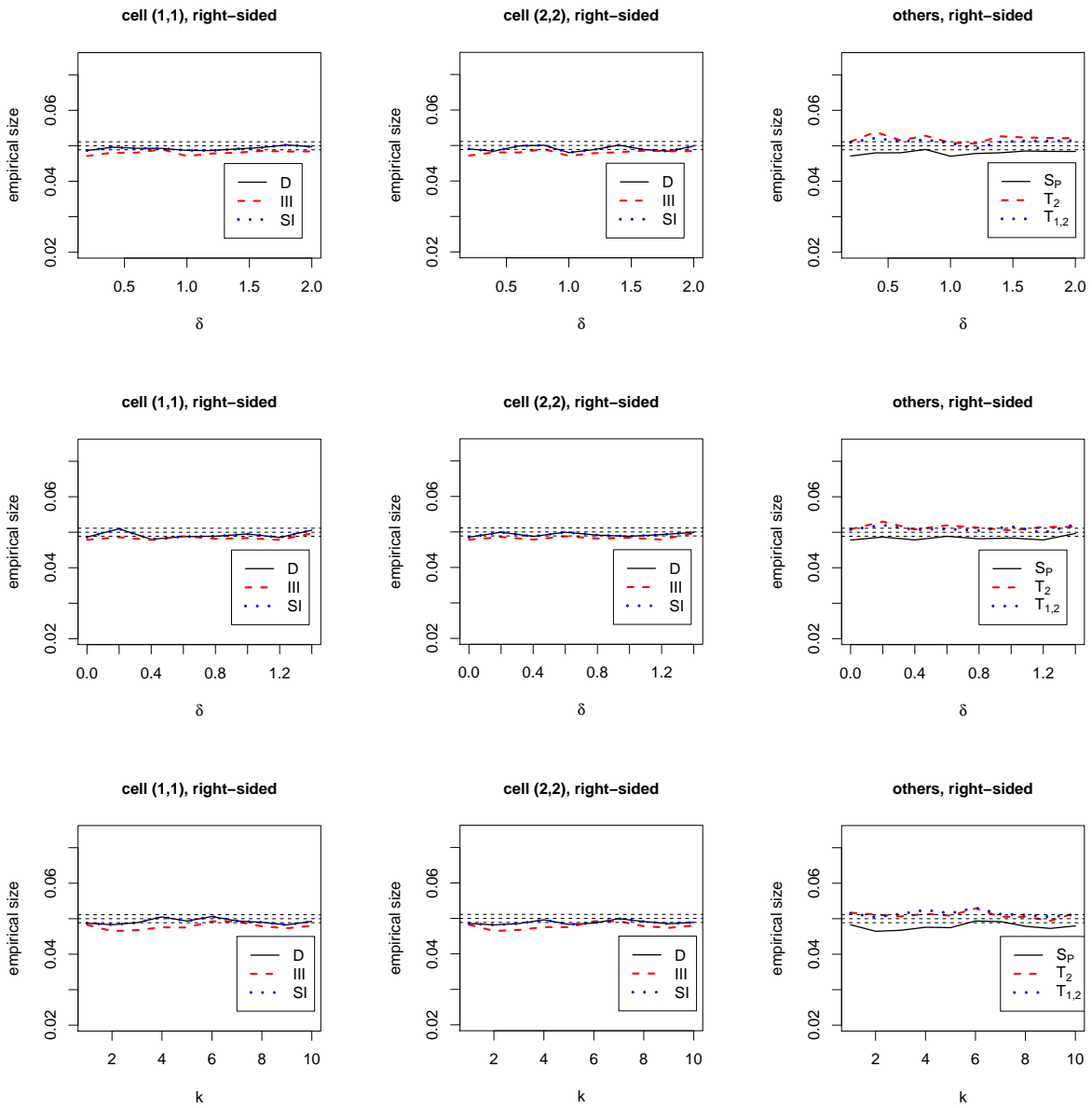


Figure 3: The empirical size estimates of the tests for the right-sided alternative under the RL cases 2-4 with $n_1 = n_2 = 100$. In case 2 (top row), we take $\delta = 0.2, 0.4, \dots, 1.4$, in case 3 (middle row), we take $\delta = 0.2, 0.4, \dots, 1.0$ and in case 4 (bottom row) we take $\delta = 0.5$ and $k = 1, 2, \dots, 5$. The dashed horizontal lines and legend labeling are as in Figure 1.

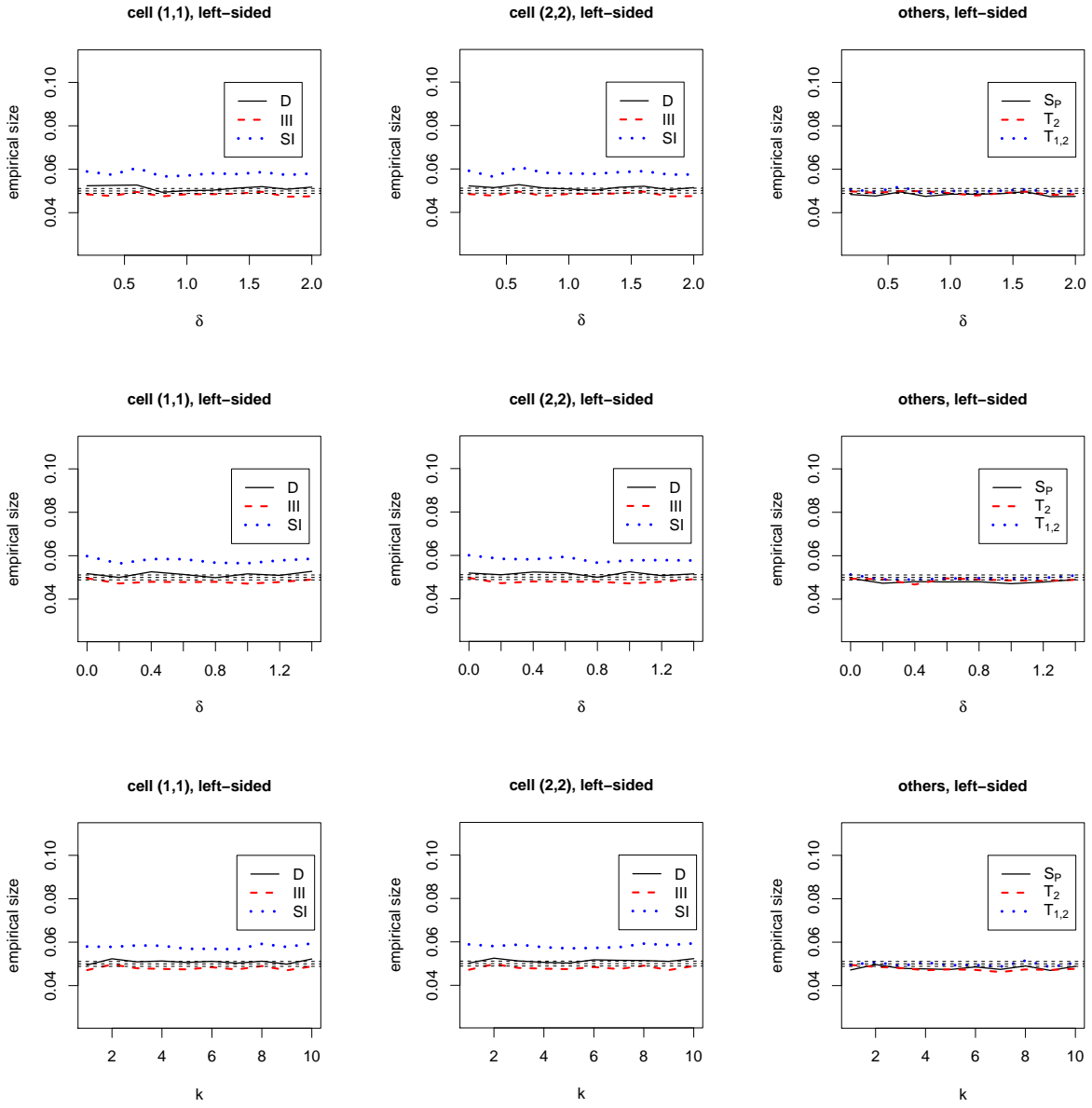


Figure 4: The empirical size estimates of the tests for the left-sided alternative under the RL cases 2 (top row), 3 (middle row), and 4 (bottom row). The dashed horizontal lines and legend labeling are as in Figure 1.

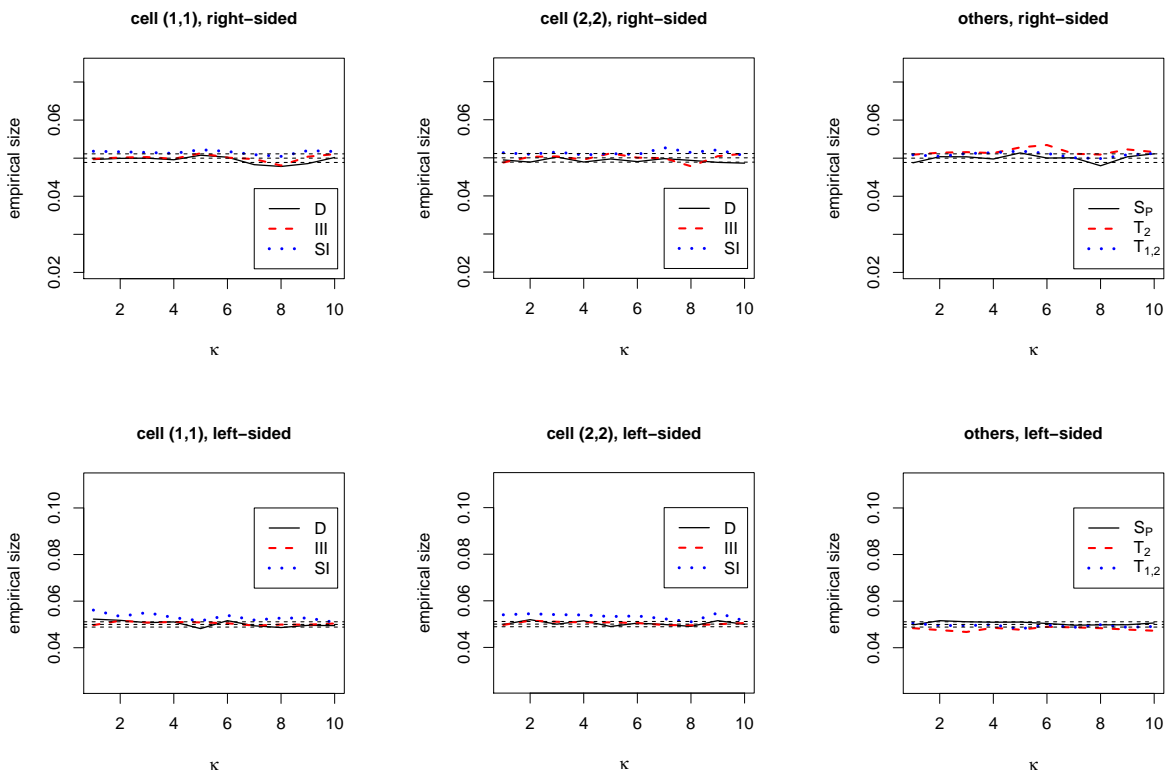


Figure 5: The empirical size estimates of the test statistics for the right-sided (top) and left-sided (bottom) alternatives under the RL case 5 with n_1 and n_2 being about half the number of generated points from the Matérn cluster process. We use $\kappa = 1, 2, \dots, 5$. The dashed horizontal lines and legend labeling are as in Figure 1.

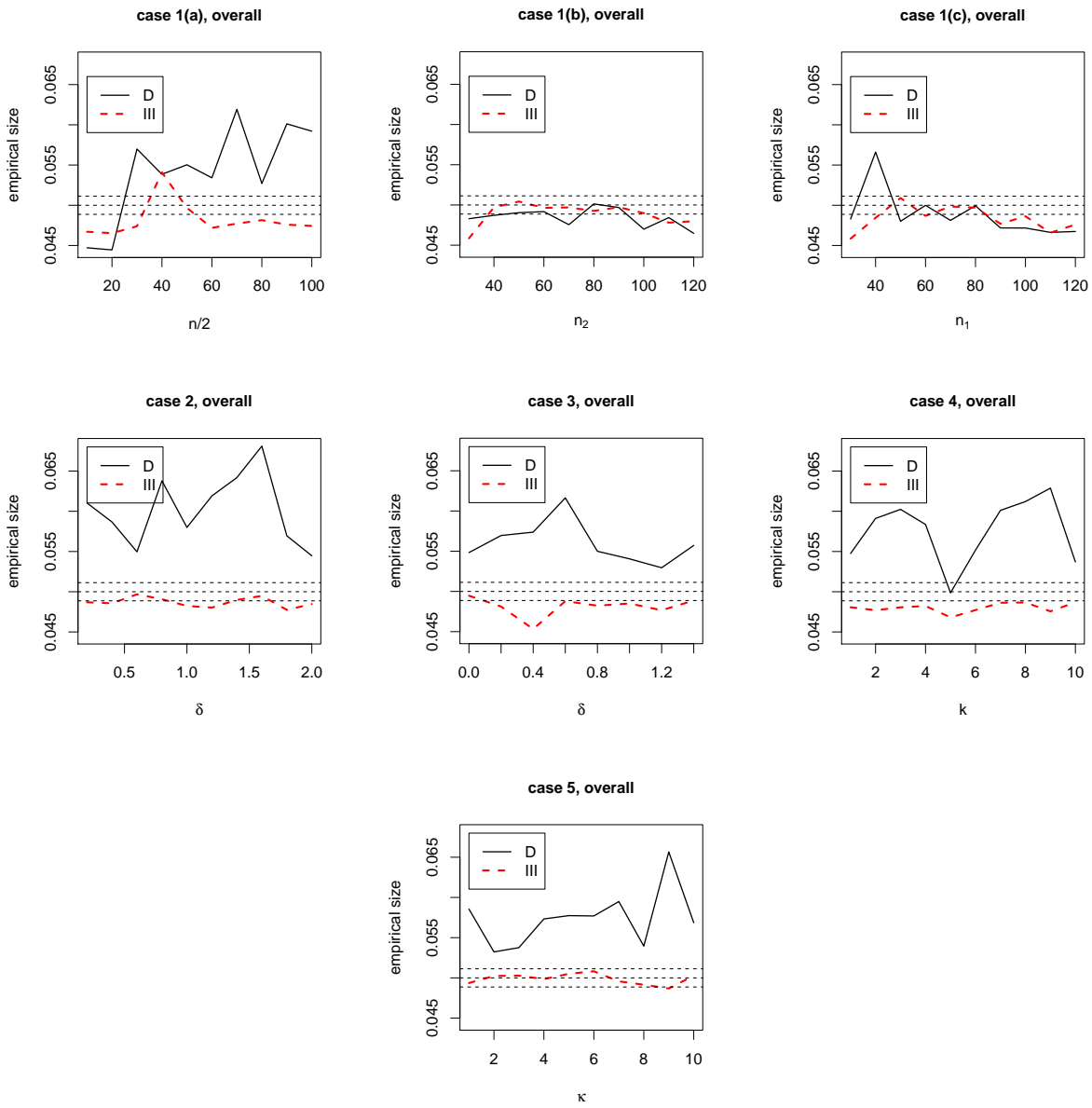


Figure 6: The empirical size estimates of the overall NNCT-tests under the RL cases 1(a)-(c) (top row in that order from left to right), and cases 2-5 (starting at second row and ordered from left to right). The dashed horizontal lines are as in Figure 1, and in the legends D stands for Dixon's overall test, and III stands for type III overall test.

compared to Dixon’s overall test. Furthermore, there is no clear trend in the size estimates as the equal sample sizes increase, or level and number of clusters increase. On the other hand, as the discrepancy between the sample sizes (i.e., differences in relative abundances) in cases 1(b) and (c) increases, the size estimates of the overall tests tend to decrease eventually.

6 Empirical Power Analysis of the Tests under Non-RL Alternatives

We propose various non-RL alternatives where case and control labels are assigned (with a pattern deviating from RL pattern) to the points generated from various homogeneous or clustering processes. In all these alternatives the background points in \mathcal{Z}_n are generated independently uniformly in the unit square $(0, 1) \times (0, 1)$, i.e., $Z_i \stackrel{iid}{\sim} \mathcal{U}((0, 1) \times (0, 1))$ for $i = 1, 2, \dots, n$. To remove the effect of one particular realization of the points on the test, we consider 100 different realizations. We only use realizations from HPP pattern for the background, because the level and number of clusters seem not to affect the size performance of the tests. Hence, in the non-RL alternatives, we only consider various non-RL schemes on the points from HPP.

Types of the Non-RL Patterns:

Case 1: Select a Z_i randomly, assign it as a case. Find its k NNs and assign them as cases with probabilities $\frac{n_1}{n} + \rho(1 - \frac{n_1}{n}), \frac{n_1}{n} + \frac{\rho}{2}(1 - \frac{n_1}{n}), \dots, \frac{n_1}{n} + \frac{\rho}{k}(1 - \frac{n_1}{n})$ until the number of cases first exceeds n_1 . We use (a) $\rho = -0.2, 0.0, 0.2, 0.4, 0.6, 0.8$ and $k = 1$ which only assigns the first NN and (b) $\rho = 0.0, 0.2, 0.4, 0.6, 0.8$ and $k = 3$ which assigns the first 3 NNs according to the above probabilities.

Case 2: In this case, we have an initial proportion, π_i , and an ultimate proportion, π_u , with $\pi_u > \pi_i$. First assign the initial proportion, π_i , of points as cases randomly and pick a case among them randomly. Then find the k NNs of this case and assign them as cases with probabilities $\rho, \rho/2, \dots, \rho/k$. Select a point randomly among these k NNs, find its k NNs and assign them as cases with the above probabilities until we have the proportion of cases first exceeding π_u . We use $\pi_i = 0.3, \pi_u = 0.5$, and $\rho = 0.2, 0.4, 0.6, 0.8$ and consider (a) $k = 1$ which only assigns the first NN and (b) $k = 3$ which assigns the first 3 NNs according to the above probabilities.

Case 3: Pick a Z_i randomly, mark it as a case and label others as a case with probabilities inversely proportional to their distances to Z_i . More specifically, we use probabilities proportional to $\frac{\rho}{k_d} \left(1 - \frac{d_{ji}}{d_{\max}}\right)^{k_p}$ where d_{ji} is the distance from Z_j to Z_i for $j \neq i$, d_{\max} is the maximum of d_{ji} values, $k_p > 0$ and $k_d \geq 1$. We stop when we first exceed n_1 cases. In our simulations we employ the usual Euclidean distance, and use (a) $\rho = 0.2, 0.4, \dots, 1.0, k_d = 1$, and $k_p = 3$, (b) $\rho = 0.8, k_d = 3, 6, \dots, 15$, and $k_p = 3$ and (c) $\rho = 0.8, k_d = 1$, and $k_p = 1, 2, \dots, 5$.

Case 4: Pick k_0 points $z'_1, z'_2, \dots, z'_{k_0}$ from \mathcal{Z}_n randomly as sources. Let φ_G be the pdf of $BVN(\mu, \sigma_1 = \sigma_2 = \sigma, \rho = 0)$ where $BVN(\mu, \sigma_1, \sigma_2, \rho)$ stands for the bivariate normal distribution with mean vector $\mu = (\mu_1, \mu_2)$, standard deviations of univariate components are σ_1 and σ_2 , and the correlation between the components is ρ . Then for each $j = 1, 2, \dots, k_0$, compute $\varphi_{G,j}(z_i)$ for all $i = 1, 2, \dots, n$ where $\varphi_{G,j}$ is the pdf of $BVN(\mu = z'_j, \sigma_1 = \sigma_2 = \sigma, \rho = 0)$ and add these pdf values. That is, find $p_G(z_i) = \sum_{j=1}^{k_0} \varphi_{G,j}(z_i)$ for each $i = 1, 2, \dots, n$. Then label the points as cases with probabilities directly proportional to the value of the pdf sums at these points. More specifically, we use probabilities $\frac{1}{p_{\max}}(p_G(z_1), p_G(z_2), \dots, p_G(z_n))$ where $p_{\max} = \max_{i=1}^n p_G(z_i)$. We stop when we first exceed n_1 cases. We use (a) $k_0 = 3, \sigma_1 = \sigma_2 = \sigma = 0.1, 0.2, \dots, 0.8$ and (b) $k_0 = 1, 2, \dots, 8$ and $\sigma_1 = \sigma_2 = \sigma = 0.4$.

We simulate 1000 Monte Carlo replications for each parameterization in each case at each background realization. For example, with a particular background realization, in case 3(a) we simulate 1000 replications for $k_p = 3$, and $k_d = 1$ and each of $\rho = 0.2, 0.4, \dots, 1.0$ with $n_1 = n_2 = 100$.

The empirical power estimates are computed similar to the empirical sizes. That is, for tests having asymptotic normality, we use the critical value $z_{.95} = 1.96$ for the right-sided alternative and $z_{.05} = -1.96$

for the left-sided alternative. And for Dixon's overall test, we use 95th percentile of the corresponding χ^2 distribution, which is $\chi_{1,.95}^2 = 3.84$ and for type III overall test, we use $\chi_{2,.95}^2 = 5.99$. Furthermore, S_{ij}^D for $i, j = 1, 2$, and the corrected versions, $S_{ij}^{D,c}$ for $i, j = 1, 2$ provide very similar empirical power estimates, hence only the former are presented.

The power estimates based on z -scores are plotted in Figures 7-10. In all these cases, Dixon's cell-specific test and segregation index for cell (i, i) provide very similar power estimates. Furthermore, we only consider right-sided alternatives, since by design, the non-RL alternatives are for segregation (or clustering of class 1) and the power estimates for the left-sided alternatives are virtually zero.

The empirical power estimates under cases 1(a) and (b) are presented in Figure 7. Notice that as ρ increases, the power estimates tend to increase as well. That is, when the probability of assigning the same label to NNs increases, the level of segregation, hence the power of the tests increases. Furthermore, the power estimates are higher for $k = 1$ (case 1(a)) compared to $k = 3$ (case 1(b)) for each test. Hence, in this type of non-RL with ρ, n_1, n_2 being fixed, as the number of NNs to be labeled increases, the power estimate tends to decrease, i.e., the level of segregation decreases. In case 1(a), among cell $(1, 1)$ statistics, Dixon's cell-specific test and segregation index have slightly higher power compared to type III cell-specific test, among cell $(2, 2)$ statistics, type III statistics have much higher power than others, and among other test statistics, Pielou's segregation index and $T_{1,2}$ have higher power. In case 1(b), among cell-specific tests, type III test has higher power, and among others, Cuzick-Edwards' tests, T_2 and $T_{1,2}$, have higher power.

We also compute empirical power estimates based on Monte Carlo critical values. Under case 1(a) of RL pattern with $n_1 = n_2 = 100$, we compute the 95th empirical percentiles of the test statistics computed in the Monte Carlo simulations and use these as the Monte Carlo critical values. For example the empirical power (based on Monte Carlo critical value) for S_P is calculated for the right-sided alternative as $\frac{1}{N_{mc}} \sum_{i=1}^{N_{mc}} \mathbf{I}(Z_{P,i} > Z_{P,crit}^{mc})$ where we have $N_{mc} = 100000$ and $Z_{P,crit}^{mc}$ is the 95th empirical percentile of the standardized version of Pielou's coefficient of segregation under RL case 1(a) with $n_1 = n_2 = 100$. The estimates for the other tests are similar. The empirical power estimates under non-RL case 1(a) based on the Monte Carlo critical values are also presented in Figure 7. We observe that the power estimates using the asymptotic critical values and those using the Monte Carlo critical values are virtually identical (this trend persists in other cases as well). Hence we only present the power estimates with the asymptotic critical values henceforth.

The empirical power estimates and the average test statistics under cases 2(a) and (b) are presented in Figure 8. In case 2(a), the power estimates are almost constant, with Cuzick-Edwards' tests having power around .80, Dixon's cell $(2, 2)$ test and index having power around .50, and all others having power around .70. In case 2(b), the power estimates are higher compared to case 1(a), and they increase as ρ increases. Among the cell-related tests, type III test has higher power (and S_P has about the same power as the type III tests). Cuzick-Edwards' tests have the higher power estimates, with T_2 having the highest power. In this type of non-RL, the power seems not to depend on ρ if only the first NN is be labeled.

The empirical power estimates under cases 3(a)-(c) are presented in Figure 9. In cases 3(a) and (b), notice that the power estimates slightly increase as ρ increases, but it seems that the power estimates (hence the level of segregation) does not crucially depend on k_d or ρ . In case 3(c), the power estimates tend to increase as k_p increases. Hence, as k_p increases, the probability of assigning the same label to NNs increases. In all these cases, among cell-specific tests, type III test has the highest power estimates, and among others T_2 has highest power.

The empirical power estimates under cases 4(a) and (b) are presented in Figure 10. In case 4(a), notice that as σ increases, the power estimates tend to decrease. That is, when σ decreases (with n_1, n_2 , and k_0 being fixed), the probability of assigning the same label to NNs of the source points increases, hence the level of segregation, thereby the power of the tests increases as well. In case 4(b), as number of source points k_0 increases, the power estimates tend to decrease. That is, when the number of source points increases (with n_1, n_2 , and σ being fixed), the (relative) probability of assigning the same label to NNs of the source points decreases, hence the level of segregation, thereby the power of the tests decreases as well. In both cases, among cell tests, type III test has higher power, and among others T_2 has higher power estimates.

The empirical power estimates of the NNCT overall tests under cases 1-4 are presented in Figure 11. The power estimates for cases 1(b), 2(b), and 3(b) are similar to those for cases 1(a), 2(a), and 3(a), respectively, hence are not presented. In all these cases, type III overall test has higher power estimates compared to

Dixon’s overall test. In cases 1(a) and (b), cases 2(a) and (b), the power estimates increase with increasing ρ (in both cases, the power estimates are higher with $k = 1$ compared to $k = 3$). In case 3(a) (resp., (b)) the power estimates does not seem to depend on the parameter ρ (resp., k_d). In case 3 (c), power estimates increase as k_p increases, in case 4(a) (resp., (b)) power estimates decrease as σ (resp., k_0) increases.

7 Example Data Sets

7.1 Childhood Leukemia Data

This data set consists of spatial locations of 62 cases of childhood leukemia in the North Humberside region of the UK, between the years 1974 to 1982 inclusive Cuzick and Edwards (1990). From the same region, a random sample of 143 controls was selected using the completely randomized design. We analyze the spatial clustering of leukemia cases with respect to controls in this data with the tests considered above. The locations of the points in the study region are plotted in Figure 12 and the segregation indices (together with standard errors) are provided in Table 2. The figure is suggestive of mild clustering of leukemia cases, and the indices together with their standard errors suggest only mild segregation (if any). Here, the indices and their standard errors are sufficient for an initial clustering assessment, since the indices either have zero expected value (as in S_P) or their expectation is approximately zero (and tending to zero with increasing class sizes) as in Dixon’s segregation indices.

Segregation Indices for Leukemia Data										
S_P	S_{11}^D	S_{22}^D	$S_{11}^{D,c}$	$S_{22}^{D,c}$						
.1348 (\pm .090)	.3548 (\pm .314)	.2362 (\pm .175)	.3420 (\pm .272)	.2317 (\pm .251)						
Test statistics for Leukemia Data										
Z_{11}^D	Z_{22}^D	Z_{11}^{III}	Z_{22}^{III}	Z_{11}^S	Z_{22}^S	Z_P	T_2	$T_{1,2}$	C_D	C_{III}
1.2021	1.2829	1.4568	1.4590	1.1292	1.3482	1.4983	2.6263	2.1206	2.2604	2.1254
associated p -values, with asymptotic critical values										
.1147	.0998	.0726	.0723	.1294	.0888	.0670	.0043	.0170	.3230	.1449
associated p -values, with Monte Carlo randomization										
.1365	.0743	.0784	.0780	.1294	.1100	.0726	.0211	.0696	.4460	.1462

Table 2: Pielou’s coefficient of segregation and Dixon’s segregation indices (\pm standard errors) together with the corrected versions and the test statistics and the associated p -values for the right-sided alternatives for North Humberside leukemia data. Z_{ii}^D (Z_{ii}^{III}) is Dixon’s (type III) cell-specific test for cell (i, i) , Z_{ii}^S is the standardized version of Dixon’s segregation indices for cell (i, i) , $i = 1, 2$, Z_P is the standardized version of Pielou’s coefficient of segregation, T_2 is Cuzick-Edward’s 2-NN test, $T_{1,2}$ is Cuzick-Edward’s combined test for $k = 1, 2$, C_D and C_{III} are Dixon’s and type III overall tests, respectively.

The appropriate null hypothesis is the RL pattern, because it is reasonable to assume that some process affects a posteriori the population of North Humberside region so that some of the individuals get to be cases, while others continue to be healthy (i.e., they are controls) Goreaud and Pélissier (2003). In Table 2, we present the test statistics and the associated p -values based on asymptotic critical values and Monte Carlo randomization. The latter is estimated as follows. The test statistics for the original data are computed, and the labels are randomly assigned to the points 10000 times. At each random assignment, we compute the test statistics, and find how many times they equal or exceed the test statistics in the original data. This number divided by 10000 yields the p -values based on Monte Carlo randomization. Notice that both versions of p -values are similar for each test (except for T_2 and $T_{1,2}$). Observe that only T_2 and $T_{1,2}$ are significant at .05 level, while all others are not. Hence, we conclude that there is no significant segregation of cases at small scales (about the first NN-distances), but cases tend to cluster significantly at larger scales. The corrected versions of the segregation indices are $Z_{11}^{D,c} = 1.2591$ and $Z_{22}^{D,c} = 1.076$ with the p -values for the right-sided alternative are .1040 and .1410, respectively. The p -values based on Monte Carlo randomization are .1294 and .1100, respectively.

Based on the tests above, we conclude that the cases and controls do not exhibit significant clustering (i.e., segregation) at small scales. Based on Cuzick-Edward’s tests, we find that the cases are significantly

segregated around k -NN distances for $k = 2$. In particular, average NN distance for leukemia data is 700 (± 1400) m, and the above analysis summarizes the pattern for about $t = 1000$ m, except for T_2 and $T_{1,2}$ where T_2 summarizes the pattern at about 1350 m (since the average 2-NN distance is 1342 m), and $T_{1,2}$ at about 1000 to 1350 m.

7.2 Liver Data

This data set consists of spatial locations of 761 cases of a liver disease in a region of interest and 3044 controls in the same region Diggle (2003). We analyze the spatial clustering of liver disease cases with respect to the healthy controls. The locations of the points are plotted in Figure 13 and provide the segregation indices in Table 3. Observe that the plot of locations is suggestive of strong clustering of cases, and the indices together with the standard errors support this initial assessment.

Segregation Indices for Liver Data										
S_P		S_{11}^D		S_{22}^D		$S_{11}^{D,c}$		$S_{22}^{D,c}$		
.0654 ($\pm .025$)		.3410 ($\pm .117$)		.0712 ($\pm .051$)		.3393 ($\pm .117$)		.0711 ($\pm .051$)		
Test statistics for Liver Data										
Z_{11}^D	Z_{22}^D	Z_{11}^{III}	Z_{22}^{III}	Z_{11}^S	Z_{22}^S	Z_P	T_2	$T_{1,2}$	C_D	C_{III}
3.2024	1.3520	3.2732	3.2729	2.9055	1.3814	2.5737	9.1854	7.7709	10.9096	10.7134
associated p -values, with asymptotic critical values										
.0007	.0882	.0005	.0005	.0018	.0836	.0050	< .0001	< .0001	.0043	.0011
associated p -values, with Monte Carlo randomization										
.0004	.0348	.0004	.0004	.0004	.0348	.0020	< .0001	< .0001	.0007	.0007

Table 3: Pielou’s coefficient of segregation and Dixon’s segregation indices (\pm standard errors) together with the corrected versions and the test statistics and the associated p -values for the right-sided alternatives for Diggle’s liver data. The labels of the tests are as in Table 2.

As in the leukemia data set, the appropriate null hypothesis is again the RL pattern. In Table 3, we present the test statistics and the associated p -values based on asymptotic critical values and Monte Carlo randomization where the latter is estimated as in Section 7.1. Both versions of p -values are similar for each test. Observe that all tests except Z_{22}^D and Z_{22}^S are significant at .05 level (but their Monte Carlo randomized versions are significant), implying significant segregation of cases at small scales (about the first NN-distances). That is, cases tend to cluster significantly at smaller scales. The corrected versions of standardized segregation indices are $Z_{11}^{D,c} = 2.9077$ and $Z_{22}^{D,c} = 1.3813$ with the p -values for the right-sided alternative are .0018 and .0836, respectively. The p -values based on Monte Carlo randomization are .0004 and .0348, respectively.

The above tests indicate a significant segregation of cases and controls and segregation of cases from controls seems to be much stronger compared to that of controls from cases. This implies a significant clustering of cases at smaller scales around the average first NN distance. Similarly, Cuzick-Edward’s tests also imply significant segregation of cases and controls around k -NN distances for $k = 2$. In particular, average NN distance for liver data is 34.24 (± 61.20), and the above analysis summarizes the pattern for about $t = 35$, except for T_2 and $T_{1,2}$ where T_2 summarizes the pattern at about 50 (since the average 2-NN distance is 52.20), and $T_{1,2}$ at about 35 to 50 units. Notice that by construction Cuzick-Edwards’ tests for T_k with $k > 1$ and T_S with $\{1\} \subsetneq S$ provide information not available by the other tests considered. However, this comes with a huge computational complexity, since for liver data it took about 7 hours to compute the Cuzick-Edwards tests T_1 , T_2 and $T_{1,2}$ in a HP Pavilion dv6 (Core i7 3720QM Processor 2.6GHz, 8GB RAM) laptop but the other NNCT-based tests took only about 5 minutes. The time difference was not that crucial for leukemia data as Cuzick-Edwards’ test took about 8 seconds, while NNCT-tests took only about .5 seconds. Our simulations indicate that NNCT-tests have $O(n^2)$ computing time, but Cuzick-Edwards’ tests for $k = 1, 2$ have $O(n^{5/2})$ computing time. Hence, when case or control sizes are large (more than a few hundred), Cuzick-Edwards’ tests are not computationally feasible, but the NNCT-tests still are.

8 Discussion and Conclusions

In this article, we propose the use of two segregation indices namely, Pielou's coefficient of segregation (Pielou (1961) and Dixon's segregation indices (Dixon (2002a)) as tests to detect segregation between two classes or in particular to detect significance of disease clustering. We derive their asymptotic distribution under RL of cases and controls to given locations, and compare these tests with some other distance-based tests (such as Dixon's cell-specific and overall tests, type III cell-specific and overall tests, Cuzick-Edwards' k -NN and combined tests) in terms of empirical size and power via extensive Monte Carlo simulations.

We investigate the effect of the clustering (i.e., level of clustering and number of clusters) of the background points (on which RL is applied) and the differences in relative abundances on the size of these tests. Our simulation results suggest that there is no increasing or decreasing trend in size when the number of clusters or level of clustering increases. On the other hand, the differences in relative abundances have much stronger influence on the size performance of the tests. We observe that Pielou's coefficient of segregation S_P , T_2 and $T_{1,2}$, and type III overall tests seem to be more robust to differences in relative abundances with S_P being the most robust. Furthermore, among cell-related and overall tests, type III tests have better size performance, and when all tests are considered Pielou's coefficient of segregation and T_2 and $T_{1,2}$ have better size performance.

We introduce four non-RL algorithms yielding clustering of cases (or segregation between the classes) after the algorithm is executed on the background points. In these non-RL alternatives, we assess the power performance of the tests, and see that type III tests and Cuzick-Edwards' tests have higher power than others (also we notice that Pielou's coefficient of segregation has power estimates close to Cuzick-Edwards' tests, although slightly lower). As for the computational complexity, Cuzick-Edwards tests require much longer time and hence not so feasible for large sample sizes, on the other hand the tests based on NNCTs require reasonable times even sample sizes are on the order of thousands.

Pielou's and Dixon's segregation indices are for testing interaction at small scales (around the average NN distance). However, our simulation study suggests that Dixon's segregation indices do not fare well in testing spatial clustering. Hence Dixon's segregation indices should not be employed with the asymptotic critical values in testing spatial clustering, but its Monte Carlo randomized version can be used. On the other hand, Pielou's segregation index performs similar to the best performing tests based on NN distances (at the scale it is intended to work, i.e., at about the first NN distance). Considering both size and power performance of the tests together, for the interaction at small scales (around the average first NN distance), we recommend type III tests (Pielou's coefficient of segregation), if the relative abundances of the classes are similar (different). For the interaction at higher scales, we recommend Cuzick-Edwards' k -NN test with $k > 1$ and combined tests T_S with $\{1\} \subsetneq S$ for testing segregation (or disease clustering) against RL with the caveat of their computational cost in time.

Acknowledgments

This research was supported by the research agency TUBITAK via Project # 111T767 and the European Commission under the Marie Curie International Outgoing Fellowship Programme via Project # 329370 titled PRinHDD.

References

- Baddeley, A. J. and Turner, R. (2005). spatstat: An R package for analyzing spatial point patterns. *Journal of Statistical Software*, 12(6):1–42.
- Bain, L. J. and Engelhardt, M. (1992). *Introduction to Probability and Mathematical Statistics, Second Edition*. Duxbury Press.
- Banerjee, S. and Dey, D. K. (2012). Editorial for the special issue on spatial statistics. *Statistical Methodology*, 9(1-2):115–116.

- Besag, J. and Newell, J. (1991). The detection of clusters in rare diseases. *Journal of the Royal Statistical Society, Series A*, 154:143–155.
- Brown, M. C. (1994). Using Gini-style indices to evaluate the spatial patterns of health practitioners: Theoretical considerations and an application based on Alberta data. *Social Science & Medicine*, 38(9):1243–1256.
- Centers for Disease Control and Prevention (1990). Guidelines for investigating clusters of health events. morbidity and mortality weekly report. 39(RR-11), 1-23.
- Ceyhan, E. (2010). New tests of spatial segregation based on nearest neighbor contingency tables. *Scandinavian Journal of Statistics*, 37:147–165.
- Ceyhan, E. (2012). New cell-specific and overall tests of spatial interaction based on nearest neighbor contingency tables. arXiv:1206.1850v1 [stat.ME]. Technical Report # KU-EC-12-1, Koç University, Istanbul, Turkey.
- Cuzick, J. and Edwards, R. (1990). Spatial clustering for inhomogeneous populations (with discussion). *Journal of the Royal Statistical Society, Series B*, 52:73–104.
- Dawkins, C. J. (2004). Measuring the spatial pattern of residential segregation. *Urban Studies*, 41(4):833–851.
- Diggle, P. J. (2003). *Statistical Analysis of Spatial Point Patterns*. Hodder Arnold Publishers, London.
- Dixon, P. M. (1994). Testing spatial segregation using a nearest-neighbor contingency table. *Ecology*, 75(7):1940–1948.
- Dixon, P. M. (2002a). Nearest-neighbor contingency table analysis of spatial segregation for several species. *Ecoscience*, 9(2):142–151.
- Dixon, P. M. (2002b). Nearest neighbor methods. *Encyclopedia of Environmetrics*, edited by Abdel H. El-Shaarawi and Walter W. Piegorsch, John Wiley & Sons Ltd., NY, 3:1370–1383.
- Eshel, G. (2012). *Spatiotemporal data analysis*. Princeton University Press, Princeton, NJ.
- Geary, R. C. (1954). The contiguity ratio and statistical mapping. *The Incorporated Statistician*, 5:115–145.
- Gómez-Rubio, V., Ferrándiz, J., and López, A. (2003). Detecting clusters of diseases with R. In *Proceedings of the 3rd International Workshop on Distributed Statistical Computing (DSC 2003) March 2002, Vienna, Austria ISSN 1609-395X Kurt Hornik, Friedrich Leisch & Achim Zeileis (eds.)* <http://www.ci.tuwien.ac.at/Conferences/DSC-2003/>.
- Goreaud, F. and Pélissier, R. (2003). Avoiding misinterpretation of biotic interactions with the intertype K_{12} -function: population independence vs. random labelling hypotheses. *Journal of Vegetation Science*, 14(5):681–692.
- Kryscio, R. J. and Lefèvre, C. (1991). Measuring the severity of disease clustering using Tango’s index. *Mathematical Biosciences*, 107(2):235–247.
- Kulldorff, M. (2006). Tests for spatial randomness adjusted for an inhomogeneity: A general framework. *Journal of the American Statistical Association*, 101(475):1289–1305.
- Kulldorff, M. and Nagarwalla, N. (1995). Spatial disease clusters: Detection and inference. *Statistics in Medicine*, 14:799–810.
- Kulldorff, M., Tango, T., and Park, P. (2003). Power comparisons for disease clustering tests. *Computational Statistics & Data Analysis*, 42:665–684.
- Lawson, A. and Denison, D. (2002). *Spatial Cluster Modelling*. CRC Press, Boca Raton, Florida.
- LeSage, J., Banerjee, S., Fischer, M. M., and Congdon, P. (2009). Spatial statistics: Methods, models & computation. *Computational Statistics & Data Analysis*, 53(8):2781–2785.
- Li, H. and Reynolds, J. F. (1993). A new contagion index to quantify spatial patterns of landscapes. *Landscape Ecology*, 8(3):155–162.

- Moran, P. A. P. (1948). The interpretation of statistical maps. *Journal of the Royal Statistical Society, Series B*, 10:243–251.
- Openshaw, S., Charlton, M., Wymer, C., and Craft, A. W. (1987). A mark I geographical analysis machine for the automated analysis of point data sets. *International Journal of Geographical Information Systems*, 1:335–358.
- Payne, L. X., Schindler, D. E., Parrish, J. K., and Temple, S. A. (2005). Quantifying spatial pattern with evenness indices. *Ecological Applications*, 15:507–520.
- Perry, J. N. (1997). Spatial association for counts of two species. *Acta Jutlandica*, 72:149–169.
- Perry, J. N. (1998). Measures of spatial pattern for counts. *Ecology*, 79(3):1008–1017.
- Pielou, E. C. (1961). Segregation and symmetry in two-species populations as studied by nearest-neighbor relationships. *Journal of Ecology*, 49(2):255–269.
- Potthoff, R. F. and Whittinghill, M. (1966). Testing for homogeneity: II. the Poisson distribution. *Acta Jutlandica*, 53:183–190.
- Ripley, B. D. (2004). *Spatial Statistics*. Wiley-Interscience, New York.
- Rogerson, P. A. (2006). Statistical methods for the detection of spatial clustering. *Statistics in Medicine*, 25:811–823.
- Searle, S. R. (2006). *Matrix Algebra Useful for Statistics*. Wiley-Intersciences.
- Song, C. and Kulldorff, M. (2003). Power evaluation of disease clustering tests. *International Journal of Health Geographics*, 2(1):9–16.
- Tango, T. (1984). The detection of disease clustering in time. *Biometrics*, 40(1):15–26.
- Tango, T. (1995). A class of tests for detecting ‘general’ and ‘focused’ clustering of rare diseases. *Statistics in Medicine*, 14:2323–2334.
- Tango, T. (1999). Comparison of general tests for spatial clustering. *Disease Mapping and Risk Assessment for Public Health, chapter 8*, pages 111–117.
- Tango, T. (2007). A class of multiplicity adjusted tests for spatial clustering based on case-control point data. *Biometrics*, 63:119–127.
- Tango, T. (2009). *Scan Statistics, Statistics for Industry and Technology, Section: Detection of Disease Clustering*. John Wiley, Chichester.
- Waller, L. A. and Gotway, C. A. (2004). *Applied Spatial Statistics for Public Health Data*. Wiley-Interscience, NJ.
- Walter, S. D. (1993). Assessing spatial patterns in disease rates. *Statistics in Medicine*, 12(19-20):1885–1894.
- Whittemore, A. S., Friend, N., Byron, W., Brown, J. R., and Holly, E. A. (1987). A test to detect clusters of disease. *Biometrika*, 74:631–635.
- Woiillez, M., Poulard, J.-C., Rivoirard, J., Petitgas, P., and Bez, N. (2007). Indices for capturing spatial patterns and their evolution in time, with application to European hake (*Merluccius merluccius*) in the Bay of Biscay. *ICES Journal of Marine Science*, 64(3):537–550.

APPENDIX

Asymptotic Approximation of Dixon's Segregation Indices when Population Proportions are Known

If the population proportion, ν_i , of class i , for $i = 1, 2$, are known, then for large n_i , we would have the following forms of Dixon's segregation index. For $i = j$, $S_{ii}^D \approx \log\left(\frac{N_{ii}}{n\nu_i - N_{ii}}\right) - \log\left(\frac{\nu_i}{1-\nu_i}\right)$. Similarly, for $i \neq j$, $S_{ij}^D \approx \log\left(\frac{N_{ij}}{n\nu_i - N_{ij}}\right) - \log\left(\frac{\nu_j}{1-\nu_j}\right)$. Then for $i = j$, letting $s \approx n\nu_i^2$ and $g(y) = \log(y/(n\nu_i - y))$, we have $g'(s) \approx \frac{1}{n\nu_i^2(1-\nu_i)} \neq 0$. By the above theorem, for large n_i , we get

$$\frac{\log\left(\frac{N_{ii}}{n\nu_i - N_{ii}}\right) - \log\left(\frac{\nu_i}{1-\nu_i}\right)}{\sqrt{\mathbf{Var}[N_{ii}]} \left(\frac{1}{n\nu_i^2(1-\nu_i)}\right)}$$

approximately having $N(0, 1)$ distribution. Similarly for $i \neq j$, letting $s \approx n\nu_i\nu_j$, we get $g'(s) \approx \frac{1}{n\nu_i\nu_j(1-\nu_j)} \neq 0$. Then for large n_i , it follows that

$$\frac{\log\left(\frac{N_{ij}}{n\nu_i - N_{ij}}\right) - \log\left(\frac{\nu_j}{1-\nu_j}\right)}{\sqrt{\mathbf{Var}[N_{ij}]} \left(\frac{1}{n\nu_i\nu_j(1-\nu_j)}\right)}$$

approximately has $N(0, 1)$ distribution.

In the two-class case (i.e., with $k = 2$), $1 - \nu_i = \nu_j$ and $1 - \nu_j = \nu_i$ for $(i, j) = (1, 2)$ and $(i, j) = (2, 1)$. So in the above expressions we can substitute these identities and reduce the expressions.

Asymptotic Distribution of the Corrected Versions of Dixon's Segregation Indices

Let $g(y) = \log\left(\frac{y+1}{n_i - y + 1}\right)$. Then $g'(y) = \frac{n_i+2}{(n_i - y + 1)(y+1)}$. For $i = j$, with $s = \frac{n_i(n_i-1)}{n-1}$, we get $g(s) = \log\left(\frac{n_i(n_i-1)+(n-1)}{n_i(n-n_i)+(n-1)}\right)$ and $g'(s) = \frac{(n_i+2)(n-1)^2}{(n_i(n-n_i)+(n-1))(n_i(n-n_i)+(n-1))}$. Hence, by Theorem 7.7.6 of Bain and Engelhardt (1992), we get

$$\frac{\log\left(\frac{N_{ii}+1}{n_i - N_{ii} + 1}\right) - \log\left(\frac{n_i(n_i-1)+(n-1)}{n_i(n-n_i)+(n-1)}\right)}{\sqrt{\mathbf{Var}[N_{ii}]} \left(\frac{(n_i+2)(n-1)^2}{(n_i(n-n_i)+(n-1))(n_i(n-n_i)+(n-1))}\right)} = \frac{S_{ii}^{D,c}}{\sqrt{\mathbf{Var}[N_{ii}]} \left(\frac{(n_i+2)(n-1)^2}{(n_i(n-n_i)+(n-1))(n_i(n-n_i)+(n-1))}\right)}$$

approximately having $N(0, 1)$ distribution for large n_i .

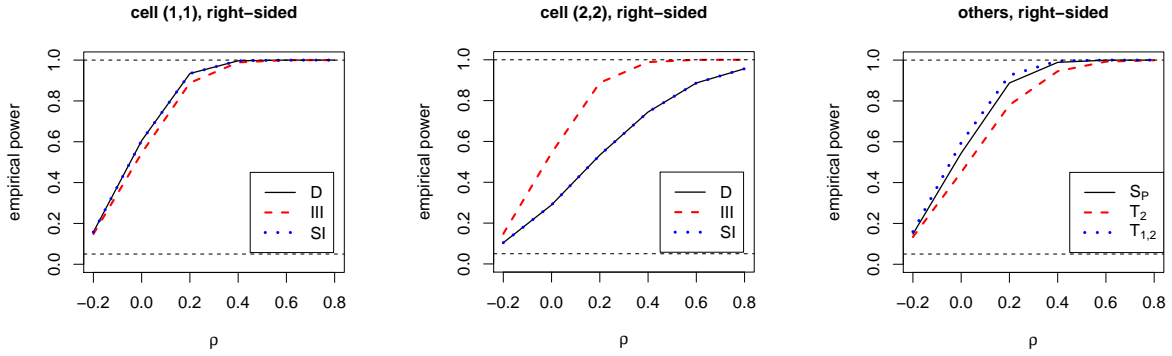
Similarly for $i \neq j$, with $s = \frac{n_i n_j}{n-1}$, we get $g(s) = \log\left(\frac{n_i n_j + n - 1}{n_i(n - n_j - 1) + (n - 1)}\right)$ and $g'(s) = \frac{(n_i+2)(n-1)^2}{(n_i n_j + n - 1)(n_i(n - n_j - 1) + (n - 1))}$. Hence, by the above theorem, we get

$$\frac{\log\left(\frac{N_{ij}+1}{n_i - N_{ij} + 1}\right) - \log\left(\frac{n_i n_j + n - 1}{n_i(n - n_j - 1) + (n - 1)}\right)}{\sqrt{\mathbf{Var}[N_{ij}]} \left(\frac{(n_i+2)(n-1)^2}{(n_i n_j + n - 1)(n_i(n - n_j - 1) + (n - 1))}\right)} = \frac{S_{ij}^{D,c}}{\sqrt{\mathbf{Var}[N_{ij}]} \left(\frac{(n_i+2)(n-1)^2}{(n_i n_j + n - 1)(n_i(n - n_j - 1) + (n - 1))}\right)}$$

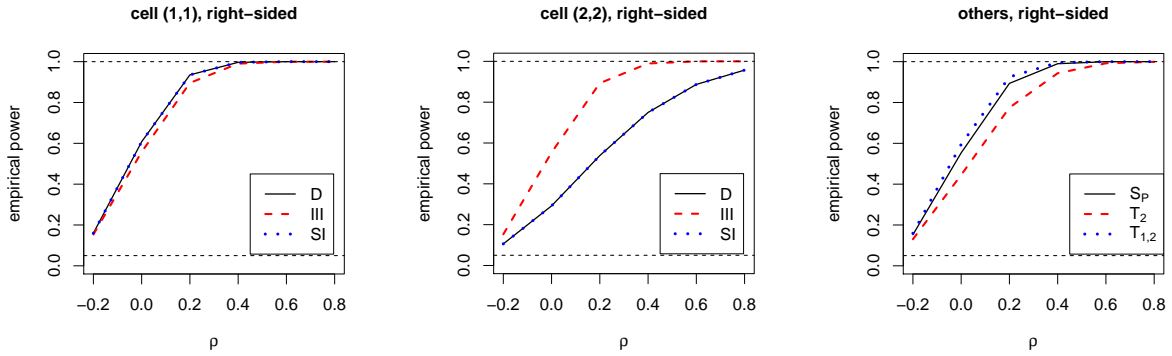
approximately having $N(0, 1)$ distribution for large n_i .

If the population proportions, ν_i , for $i = 1, 2$ are known, the corrected and uncorrected versions are equivalent as the class sizes tend to infinity.

Power Estimates for Case 1(a) with Asymptotic Critical Values



Power Estimates for Case 1(a) with Monte Carlo Critical Values



Power Estimates for Case 1(b) with Asymptotic Critical Values

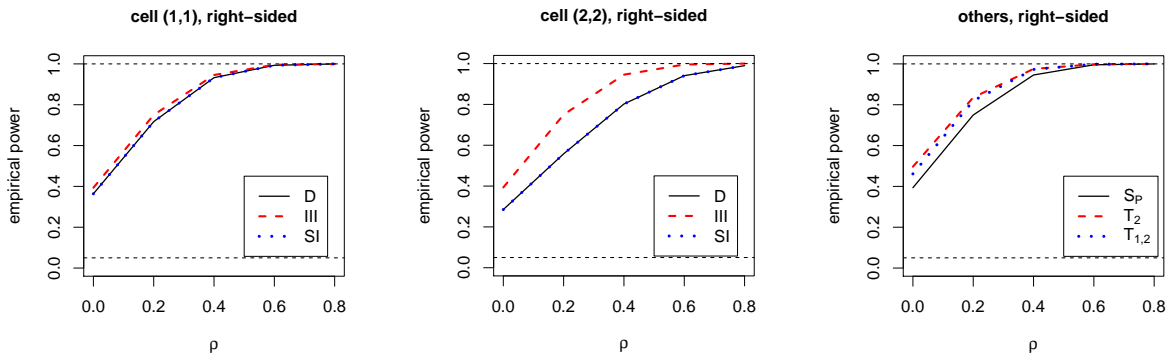


Figure 7: Empirical power estimates under the non-RL cases 1(a)-(b). In case 1(a) (top row), we take $\rho = -0.2, 0.0, 0.2, \dots, 0.8$ and $k = 1$ and in case 1(b) (bottom row), we take $\rho = 0.0, 0.2, \dots, 0.8$ and $k = 3$. The dashed horizontal lines are at 0.05 and 1.0 and legend labeling is as in Figure 1.

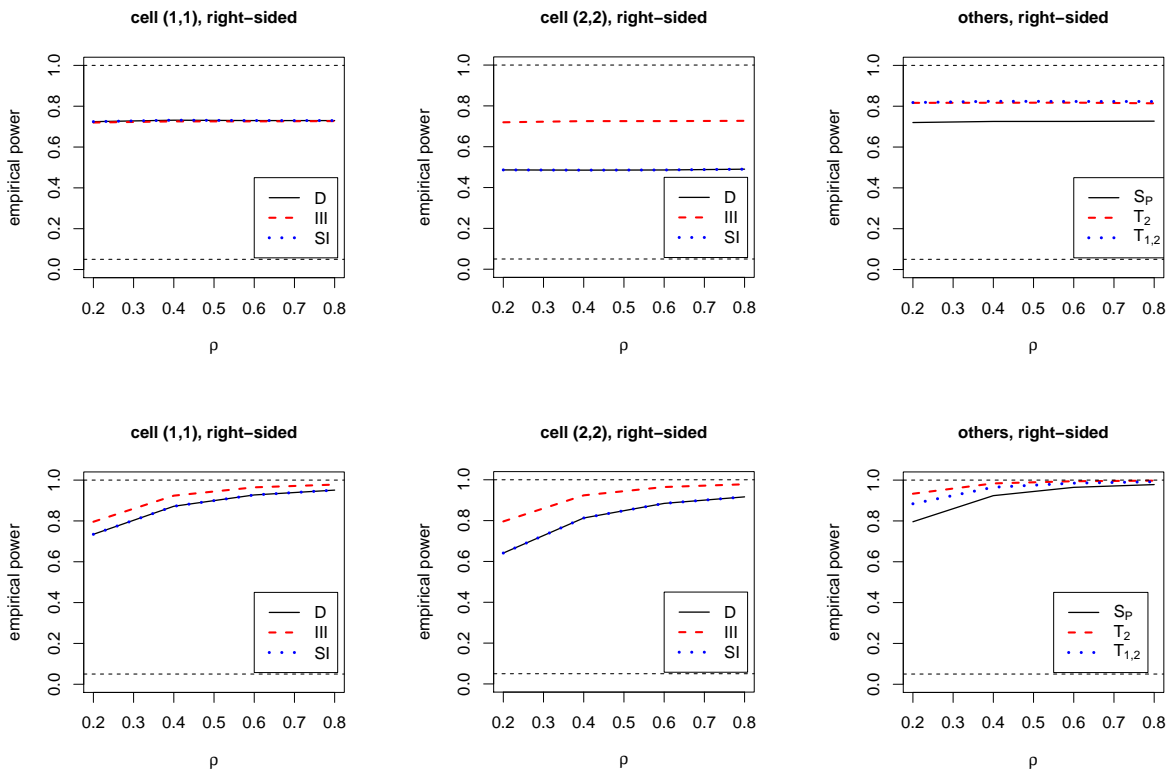


Figure 8: Empirical power estimates under the non-RL case 2(a) (top row) and case 2(b) (bottom row) with $\pi_i = 0.3$, $\pi_u = 0.5$, $\rho = 0.2, 0.4, 0.6, 0.8$. The dashed horizontal lines and the legend labeling in both rows are as in Figure 7.

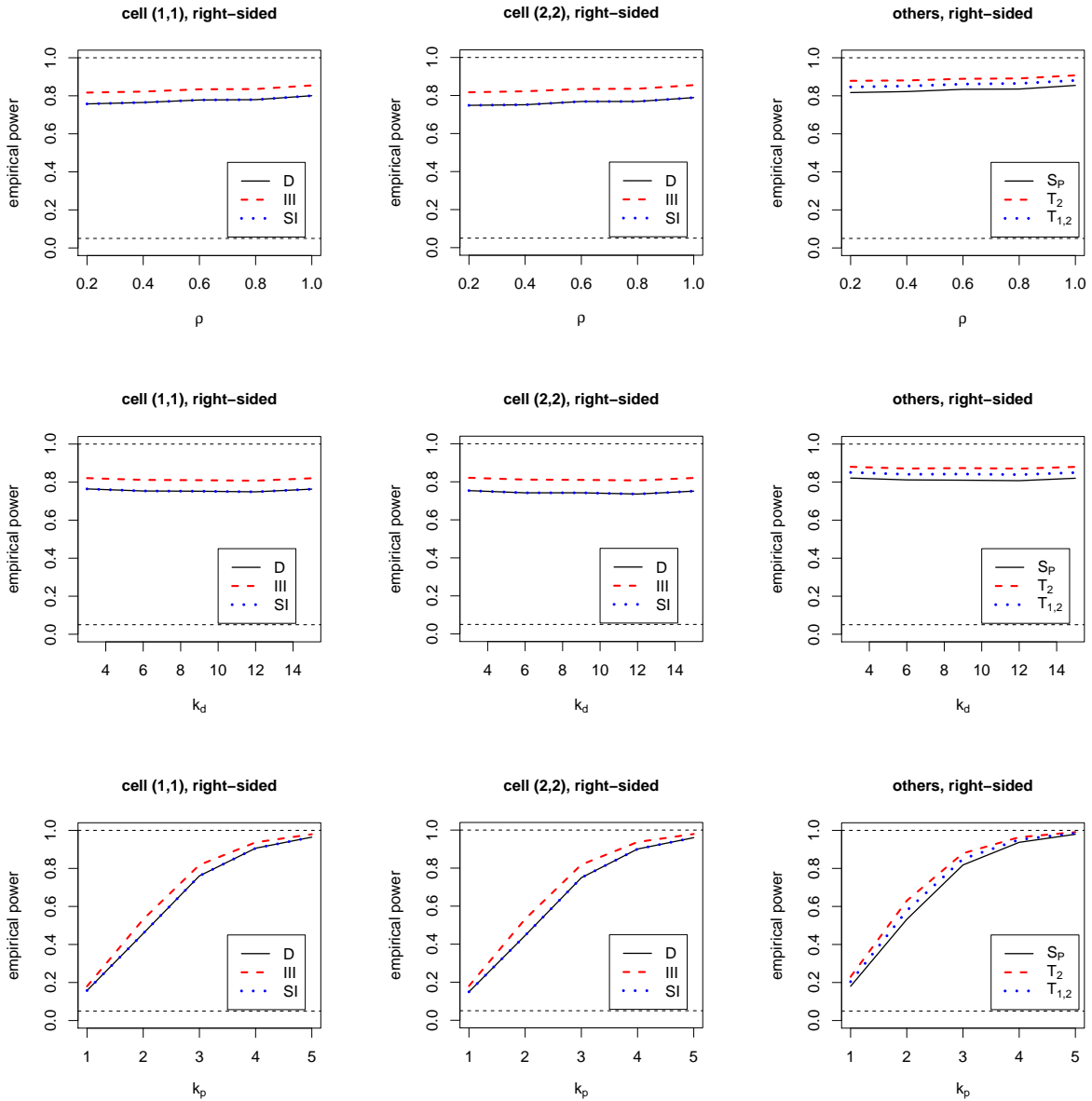


Figure 9: Empirical power estimates under the non-RL cases 3(a)-(c). In case 3(a) (top row), we take $\rho = 0.2, 0.4, \dots, 1.0$, $k_p = 3$, and $k_d = 1$, in case 3(b) (middle row), we take $\rho = 0.8$, $k_p = 3$, and $k_d = 3, 6, \dots, 15$, and in case 3(c) (bottom row) we take $\rho = 0.8$, $k_p = 1, 2, \dots, 5$, and $k_d = 1$. The dashed horizontal line and legend labeling are as in Figure 7.

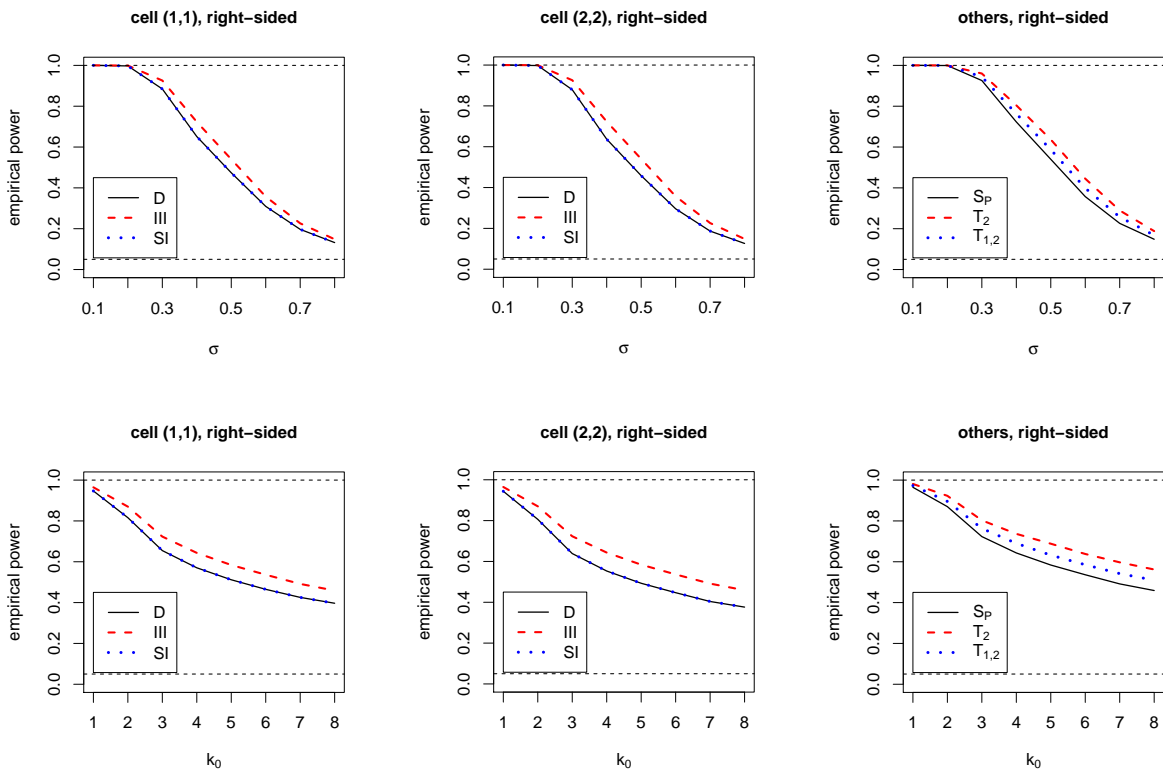


Figure 10: Empirical power estimates under the non-RL cases 4(a)-(b). In case 4(a) (top row), we take $k_0 = 3$ and $\sigma = 0.1, 0.2, \dots, 0.8$ and in case 4(b) (bottom row), we take $k_0 = 1, 2, \dots, 8$ and $\sigma = 0.4$. The dashed horizontal line and legend labeling are as in Figure 7.

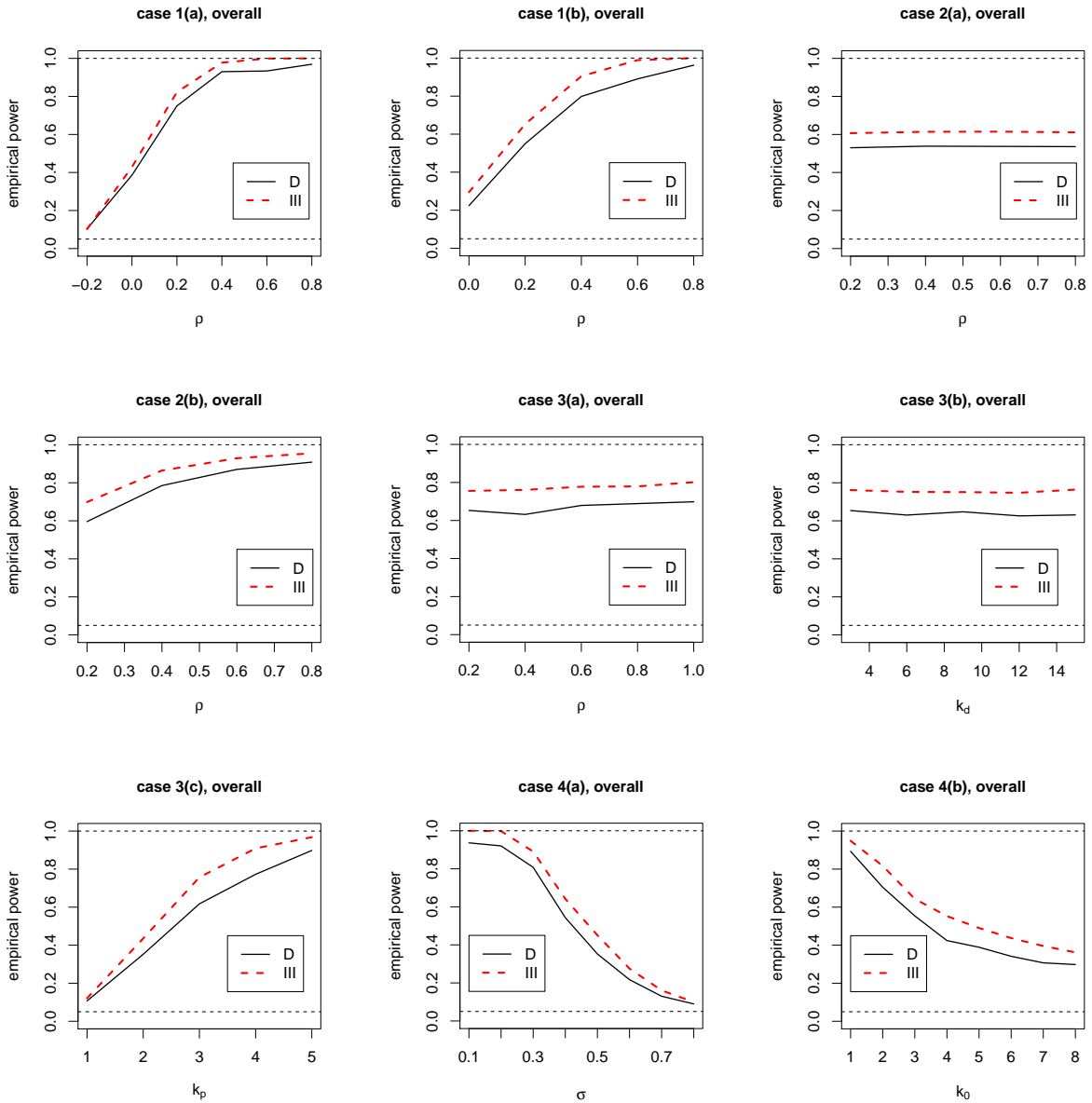


Figure 11: Empirical power estimates for the overall NNCT-tests under the non-RL cases 1-4. D stands for Dixon's overall test and III stands for type III overall test.

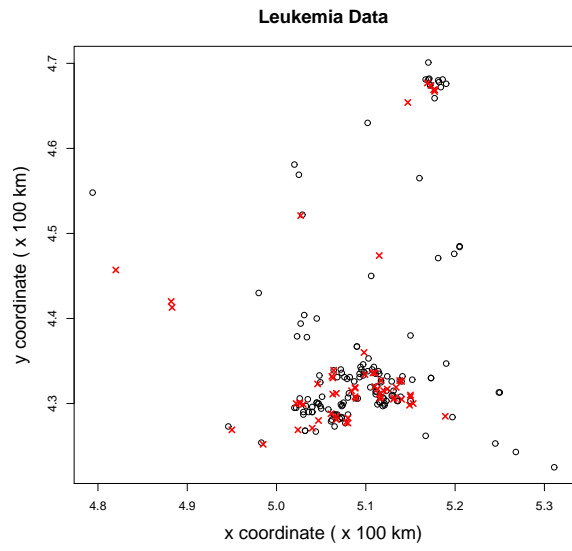


Figure 12: The scatter plots of the locations of cases (crosses \times) and controls (circles \circ) in North Humberside leukemia data set.

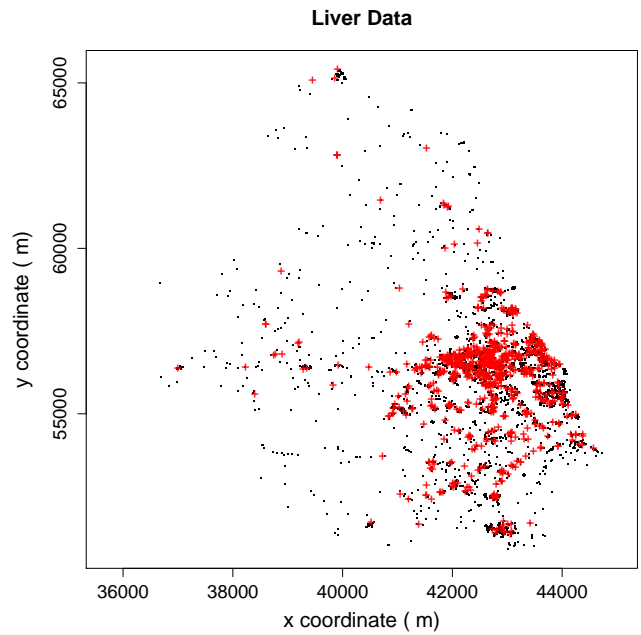


Figure 13: The scatter plots of the locations of cases (pluses $+$) and controls (dots \cdot) in Diggle's liver data set.